Challenges and Perspectives in the Development of Polymer-based Nanoparticles for Efficient Intracellular Delivery of Exogenous RNA: A Literature Review

Word count: ~6650

Silvia Smith (stxss56@nottingham.ac.uk)

University of Nottingham, School of Biosciences,

Sutton Bonington,

LE12 5RD

MRes Biomolecular Technology

Supervisor: Professor Cameron Alexander

Contents

Abstract

The approval of two mRNA vaccines for COVID-19 by the U.S. FDA generated significant attention from the scientific community for RNA technology, with its safety, efficacy, and rapid production capabilities. Beyond infectious disease, RNA therapeutics hold great promise in cancer treatment and various other diseases. However, the physiochemical properties of free mRNA present significant challenges in achieving efficient intracellular delivery *in vivo*. Therefore, the development of effective delivery systems for exogenous RNA is crucial. Among various delivery methods, lipid and polymer-based nanoparticles (LNPs and PNPs) have emerged as prominent candidates.

This review discusses different classes of PNPs, providing a comprehensive analysis of their molecular design criteria and plausible internalisation pathways within cells. Despite, their favourable pharmacokinetics, precise tunability of chemical properties, and potential for cellular targeting, PNPs are behind LNPs in clinical advancement. This review explores the key challenges encountered in PNP development, with a particular emphasis on the importance of understanding PNP endosome escape mechanisms, which currently represent a bottleneck for improving transfection efficiency. By identifying how PNP composition, shape, and size influence endosome escape, PNP formulations can be optimised to deliver RNA therapeutics effectively and safely. Future perspectives and research directions necessary for the clinical translation of PNPs are also discussed.

1. Introduction.

Since the successful FDA (U.S. Food and Drug Administration) authorisation and release of the Pfizer and Moderna COVID-19 messenger RNA (mRNA) vaccines, the advancement of RNA therapeutics has developed rapidly. RNA vaccines provide the host with the means to complete mRNA-mediated expression of an antigen which, therein, activates a long-lasting immunity against the pathogen. This breakthrough technology has gained significant global recognition as it has the potential to transform medicine with other possible applications including cancer treatments (mRNA-encoded melanoma-associated antigens (Sahin *et al.*, 2020)), protein replacement therapies (cystic fibrosis (Miah, Hyde and Gill, 2019)) and gene editing therapies (mRNA encoded DNA nucleases (Finn *et al.*, 2018)) (Yang *et al.*, 2023).

Theoretically, specfic sequences of mRNA can be produced to enable the expression of virtually any protein *in vivo*. The host cells and their translational machinery are utilised for protein production. For mRNA vaccines, an immune response is activated whilst also avoiding the risks associated with traditional vaccine methods containing weakened or dead viruses. For protein replacement therapies, this utilisation of host resources helps apply the appropriate post-translational modifications required to reduce immunogenicity and improve functionality (Barbier *et al.*, 2022).

Therefore, there is now an increasing requirement for the adjacent development of potent, specific, and safe methods for mRNA delivery. With RNA being negatively charged, it has been identified to complex with either positively charged lipids or other polymers, under the appropriate conditions, to form a micelle structured nanoparticle (Paunovska *et al.*, 2022).

Currently, most of the research covers lipid-based nanoparticles (LNPs) for RNA delivery. Advanced investigations have confirmed the safety and potent transfection ability of PNPs. However, these studies have also identified certain limitations, including thermostability issues (requiring costly cold chains and logistics), and in numerous instances, high levels of cytotoxicity (Yang *et al.*, 2023). Rapidly gaining more attention, polymer-based nanoparticles (PNPs) are emerging as a new possibility for mRNA delivery. Despite being less advanced clinically than lipids and having unique challenges of their own, PNPs have the potential to provide novel features. For example, some PNPs can assemble in aqueous conditions, exhibit long-term stability during storage, and possess unique pharmacokinetic properties. These characteristics make them promising candidates for development of delivery systems for advanced mRNA therapies. Also, with carefully tuned chemical features, PNPs could provide the unique ability and unprecedented opportunity to manage effective mRNA transport and protection, enabling the stable transfection of cells (Yang *et al.*, 2023).

To achieve a global approval of PNPs, more must be understood about the various mechanisms that underly their cellular internalisation, from uptake into cellular compartments to their escape into the cytosol. Only then, can the specific PNP properties and structures responsible for improving various transfection stages be identified. This is necessary for optimising effective PNP design (Sunshine, Peng and Green, 2012).

A a high proportion of the administered PNPs remain in cellular endosomes and lysosomes for degradation (Patel *et al.*, 2017), failing to deliver the mRNA to the cytosol. Therefore, the limiting factor impeding mRNA delivery and successful transfection is the escape from entrapment within endosomes. However, there is currently limited scientific consensus about the mechanisms of endosome escape used by PNPs. Therefore, this review aims to address the conflicting reports published about the more widely accepted "proton sponge" hypothesis, whilst considering other mechanisms including polymer swelling and those utilised by LNPs. Other additional factors that influence the transfection efficiency of PNPs are covered also.

It is of immediate importance to uncover how the universal design of PNPs relates to their structure-function relationship with biological systems, diseased cells and tissues (Mendes *et al.*, 2022). The ongoing study and development of formulation science with RNA delivery systems is therefore just as important for the future of RNA therapeutics as understanding the properties and biology of RNA itself. Furthermore, developing a better understanding of how PNPs escape endosomes is essential for improving this key step in transfection.

2. RNA therapeutics

2.1 The potential of RNA.

The main attraction of RNA therapeutics is that only a single sample of genetic material is required to generate a durable transgene expression and subsequent successful treatment for a patient (Deverman *et al.*, 2018). With other existing biopharmaceuticals, there is a time and cost associated with the carefully controlled environments and extensive purification procedures required for their production (Taylor, 2015). However, in principle, RNA therapeutics bypasses these challenges as the delivered mRNA mimics the fully mature, native mRNA and utilises the translational machinery of the host to express the desired protien. As this all occurs *in vivo*, less manufacturing steps are required to obtain the final therapeutic outcome (e.g. protein replacement treatment or immunisation (Zhu *et al.*, 2022)).

Moreover, RNA is the therapeutic of choice, over DNA, as there is no need for nuclear entry and localisation or transcription. Instead, RNA is translated immediately once it reaches the cytoplasm, hence accelerating protein production (Herndon, Quirk and Nilson, 2016). Also, there is no risk of irreversible integration into the genome or mutagenesis between host and therapeutic DNA, avoiding genotoxicity (Huang *et al.*, 2022). Other forms of RNA are also being explored as therapeutics, including small interfering (siRNA) and microRNA (miRNA), both of which are involved in RNA silencing and post-transcriptional regulation of gene expression (Mendes *et al.*, 2022).

After translation of the exogenous mRNA, the free nucleic acid sequence is readily degraded in the cytosol, with a half-life ranging from several minutes to hours depending on various factors with the specific mRNA (Schoenberg and Maquat, 2012). This is beneficial for preventing the long-term build-up of material but also provides challenges of its own for applications concerning long-term protein replacement.

2.2 A delivery vehicle is required.

There is no simple, direct delivery of nucleic acids into a desired cell, because of low *in vivo* stability, rapid host degradation prior to cell entry and failure to pass through the extracellular matrix and cellular lipid bilayer (Zhu *et al.*, 2022). Molecules of mRNA are usually degraded within minutes by nuclease enzymes (RNase) in the bloodstream. As most mRNA degradation starts at the 3' polyadenine tail and the 5' cap (Liu, Liang and Huang, 2021), certain chemical modifications extending the 3' polyadenine tail or altering the 5' cap can improve mRNA stability. However, this fails to provide the assistance required for effective RNA transportation across cell membranes. Their delivery inside the cell is challenging owing to their negative charge, high molecular weight (~600 – 8,000kDa for self-replicating mRNAs (Dowdy, 2017), and hydrophilicity of nucleic acids all preventing cellular membrane permeability (Mendes *et al.*, 2022). The large secondary structure of single-stranded mRNA is much larger compared to other approved small-molecule drugs that can access cells.

Therefore, despite some of these challenges being partially resolved by chemical modification to the RNA molecule itself (Wadhwa *et al.*, 2020), a well-designed delivery vehicle is required to simultaneously package RNA compactly, facilitate nucleic acid delivery (sometimes into specific, target cells), and protect RNA cargo from degradation. Once inside the cell, the delivery vessel should then also promote endosomal escape to effectively deliver the RNA to the host ribosomes to translate the relative therapeutic (Sung and Kim, 2019). It goes without saying, the delivery mechanism must also avoid immunorecognition.

Another advantage of having a suitable delivery system is that the amount of chemical modifications made to the specifically curated RNA sequence can be reduced (Mendes *et al.*, 2022). Furthermore, the delivery vehicle provides an opportunity to control the localisation and durability of RNA release, as required (Kamaly *et al.*, 2016).

3. Nanoparticle development

3.1 Nanoparticles complex with RNA cargo.

After acknowledging the therapeutic potential of RNA, scientists began to explore various ways in which to successfully deliver mRNA directly to cells. As expected, administering free, unprotected mRNA failed to transfect cells owing to its susceptibility to extracellular degradation. This triggered the exploration of protecting RNA by condensation into nanoparticles.

Viral vectors were initially considered due to their promising cellular uptake efficiency, but it was also recognised that many modifications would be required to prevent risks of inducing the host inflammatory and immune response. These safety issues can be evaded by utilising the promising, non-viral vehicles made up of predominantly lipids or polymers (Tros de Ilarduya, Sun and Düzgüneş, 2010). For successful transfection, nanoparticles of this kind tend to be less than 100nm in diameter (Yang *et al.*, 2023).

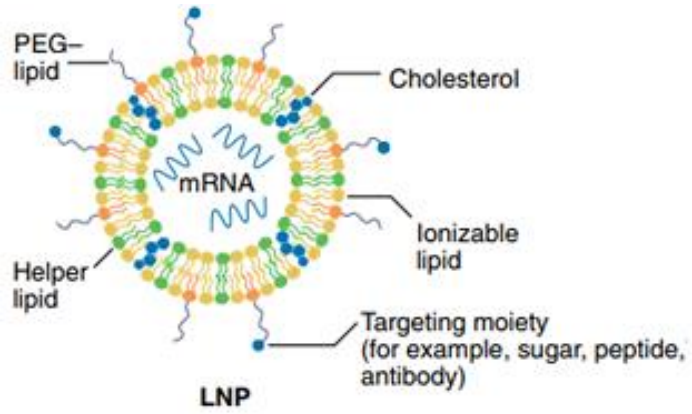

Figure. 1. *Generic LNP-mRNA complex structure, including various modifiable components* (Barbier *et al.*, 2022).

Due to the universally approved COVID-19 mRNA vaccine that is packaged into LNPs, the lipid-based delivery systems are the more widely investigated. Entrapment of RNA into LNPs is achieved by a charge-driven interaction between the positively charged lipids and polyanionic nucleic acid. A near-neutral surface charge desirable for clinical administration is then achieved by adjusting the pH to

above the pKa of the ionisable lipid (Gindy *et al.*, 2014; Brader *et al.*, 2021). LNP formulations possess four main components: the cationic, ionisable lipids that form complexation with; a helper phospholipid, resembling those found in the cell membrane, to promote bilayer structure; a cholesterol equivalent to regulate the fluidity of the lipid bilayer; and a polyethylene glycol (PEG)-lipid to enhance colloidal stability and decrease opsonisation by shielding any residual surface charge (Barbier *et al.*, 2022). *Figure 1* shows a representation of the arrangement of these components in an LNP, while *figure 2* shows the chemical structures of some commonly used components.

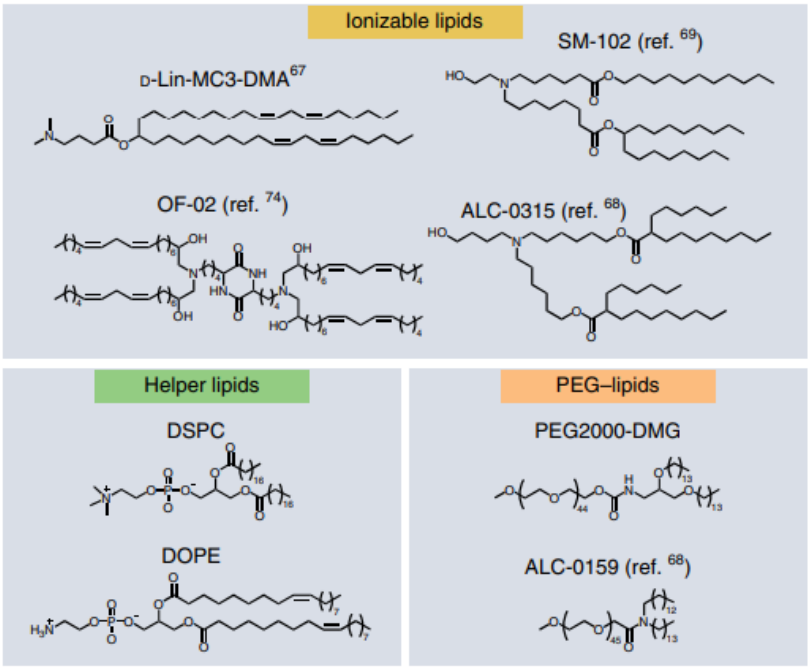

Figure. 2. *Common lipid structures used for LNP design.*

For PNP formulations, the cationic lipids are often replaced with biodegradable, amine containing polymers that can also, self-assemble with RNA (Barbier *et al.*, 2022). Poly(beta-amino ester)s (PBAEs) are one such cationic polymer class. PBAEs are characterised by the presence of cationic amines and biodegradable ester bonds (Choi *et al.*, 2020; Paunovska *et al.*, 2022). Like LNPs, chemical modification to the polymers can improve PNP efficacy and tolerability *in vivo*. However, unlike cationic lipids, few nanoparticle formulations using polymeric materials are currently used for the delivery of therapeutic nucleic acids (Kowalski *et al.*, 2019) as more research is required.

3.2 Lipid-based nanoparticles

Lipid-based nano-delivery systems are currently the most widely used and at the forefront of clinical translation of RNA therapeutics, this having intensified after their use for the approved COVID-19 mRNA vaccines. They provide effective for protection against RNase degradation during systemic

circulation allowing cellular uptake and transportation of the mRNA from the early endosome into the cytosol via fusion with the lipid bilayer (Hou *et al.*, 2021; Ramachandran, Satapathy and Dutta, 2022). Studies have demonstrated how lipid structure and ratios affect LNP interactions with cells, and crucially, the cell in which it targets (Semple *et al.*, 2010). For vaccines, targeting delivery towards specific tissues or cells is less important than other RNA therapies provided the mRNA is translated to activate the immune system appropriately.

The ionisable lipid component of the LNP is of most importance for its key role in particle formulation, cellular uptake, and endosomal escape (Han *et al.*, 2021). There are substantial differences between the structural diversity of cationic or ionisable lipids amongst existing LNP formulations. Therefore, high-throughput techniques for synthesising extensive libraries of novel lipids and assessing their effectiveness *in vitro* and *in vivo* have been developed to expedite the discovery of potent, ionisable lipid structures (Li *et al.*, 2023).

Technological advances in LNP design have focussed heavily on incorporating hydrolysable bonds to encourage LNP degradation post-transfection to prevent an accumulation of lipids. Precautions must be taken where repeat dosing may be required as this could lead to lipid accumulation within tissues. Little is known about potential long-term risks. It is important to prevent any risk of cell autonomous toxicity (Paramasivam *et al.*, 2021) and in the case of non-vaccine therapeutics, non-cell-autonomous (e.g. inflammation) responses. However, the compromise of having more degradable bonds is a reduction in formulation stability. This continues to be the greatest challenge for LNP formulations (Barbier *et al.*, 2022).

3.3 Polymer-based nanoparticles

Despite being less clinically advanced than LNPs, PNPs also show exciting potential as delivery systems. They both share some similar physiochemical characteristics and like LNPs, PNPs can also be modified to modulate RNA delivery into cells. These tuneable polymer structural characteristics include surface (net) charge, degradability, molecular weight, hydrophobicity and polydispersity (Paunovska *et al.*, 2022). Optimising the chemical structure of the monomer is key for successful PNP development (Kamaly *et al.*, 2016).

However, polymer-based delivery systems have taken longer to develop than lipid-based delivery systems owing to their greater polydispersity, the toxicity of cationic polymers and challenges associated with the metabolism of large molecular weight polymers (Kowalski *et al.*, 2019; Ramachandran, Satapathy and Dutta, 2022).

3.3.1 Classes of PNP.

The amine groups of the cationic polymers electrostatically bind to the negatively charged nucleic acids (*as demonstrated in Figure 4*) to produce relatively compact polyplexes (Zhu *et al.*, 2022). It was recognised that certain classes of cationic polymers, including polyethyleneimine (PEI), poly(l-lysine) (PLL) and PBAE are capable of this condensation reaction with RNA molecules, successfully enabling their delivery into cells. Hence, PNPs are being explored as alternative vaccine delivery candidates. PNPs are generally smaller than cationic liposomes, theoretically also improving potential cellular uptake and transfection efficacy (Tros de Ilarduya, Sun and Düzgüneş, 2010).

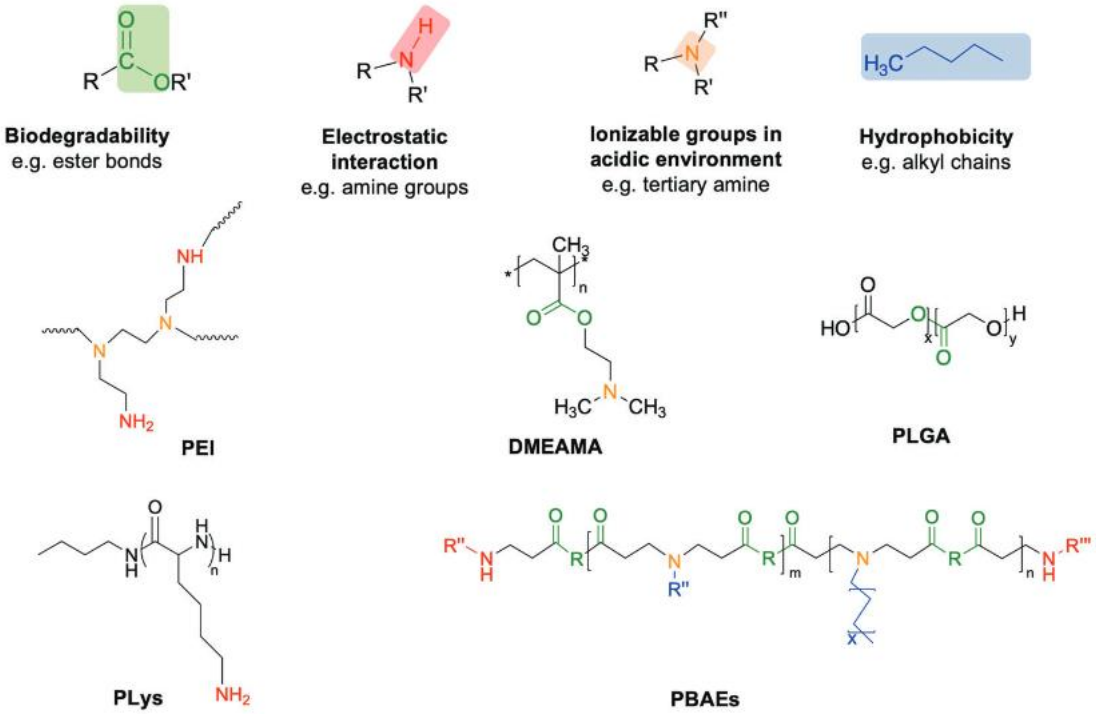

Figure. 3. *Overview of the design elements that constitute the various PNP classes and are ideal components for improving delivery efficiency* (Yang *et al.*, 2023).

The general chemical properties required for effective PNP design are highlighted in *figure* 3. It is important for PNPs to form stable complexes with RNA whilst also being biodegradable to reduce cytotoxic effects. Polymers with chemical structures that increase PNP hydrophobicity and protonation in acidic environments are considered to improve endosomal escape through mechanisms discussed in *Section 4.4*.

Besides RNA therapeutics, regulatory authorities (FDA and European Medicines Agency) have approved various polymers for the delivery of small-molecule drugs (Choi and Han, 2018). One example is the extensively researched synthetic biodegradable poly(lactic-co-glycolic acid) (PLGA). Polymers of the PLGA (*figure 3*) class possess the ideal biodegradation kinetics, toxicological profile,

drug loading efficacy and mechanical properties necessary for drug delivery (Duncan, Ringsdorf and Satchi-Fainaro, 2006). However, PLGA polymers are not employed directly for RNA delivery due to their inherent lack of positive charge, which is essential for complexing anionic RNA at a neutral pH. One potential solution to this limitation involves chemically modifying PLGA. Chemists typically engineer PLGA to incorporate distinct cationic chemical groups, such as chitosan, to successfully form complexes between modified PLGA with RNA (Xiao *et al.*, 2016). Further studies are required to test how this affects transfection efficacy *in vivo* and *in vitro*.

The PEI family is the most widely studied of the cationic polymers used for RNA delivery. They consist of linear or branched polycations that have a strong affinity for various forms of nucleic acids (Akinc *et al.*, 2005), generating nanoscale complexes. Despite protecting and delivering RNA successfully *in vitro* (Zhu *et al.*, 2022), PEI is relatively cytotoxic and non-biodegradable, preventing its utilisation *in vivo* (Pandey and Sawant, 2016). Unmodified PEI is therefore used primarily as a positive control for successful transfection when testing novel PNPs *in vitro*. The associated high toxicity with PEI has been the major motivation for testing PEI modifications and the exploration of other polymer vectors.

As PEI and PLL are naturally cationic, they do not require the addition of cationic chemical groups to electrostatically bind mRNA (*figure 4*). However, it is important to find the right balance between transfection capability and toxicity as both are increased with the molecular weight of these polymers. There are a number of possible modifications that aim improve their in vivo efficacy, colloidal stability and tolerability. (Paunovska *et al.*, 2022).

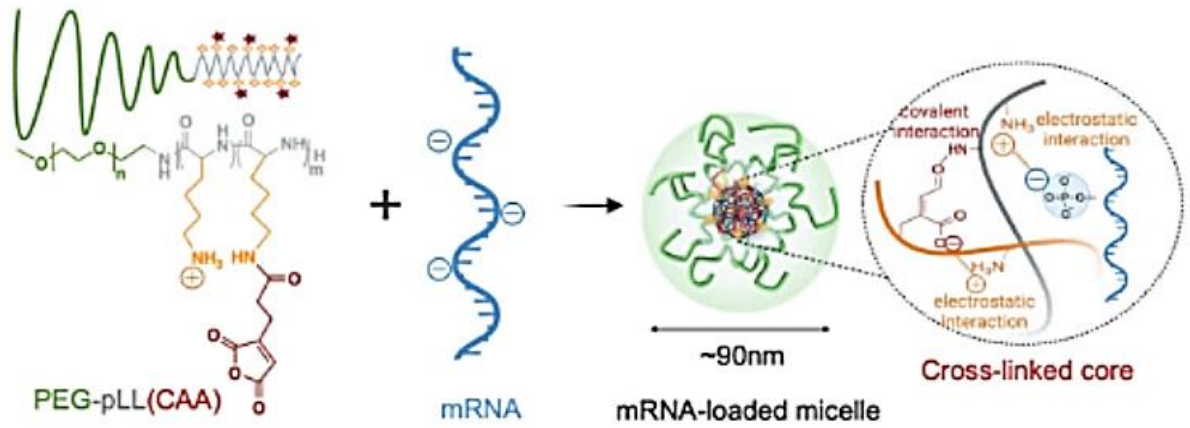

Figure. 4. *The complexation of an example, modified polymer (PLL) with mRNA via electrostatic interactions to generate a carrier vehicle* (Yang *et al.*, 2023)**.**

To address these limitations, PNPs can be modified by surface-functionalised polyethylene glycol (PEG)ylation (*figure 5*). For example, PEG-*grafted*-PEI effectively delivered DNA to pulmonary immune cells, showing lower toxicity than the non-PEGylated PEI (Ke *et al.*, 2020). Or, to provide a modification

example using RNA, conjugating PEI to cyclodextrin enabled the successful delivery of an mRNA vaccine *in vivo*. Coupling cyclodextrin to PEI allows a delocalisation of the polyamine backbone charge density, thereby reducing cytotoxicity while preserving available protonatable groups (Tros de Ilarduya, Sun and Düzgüneş, 2010; Tan *et al.*, 2020). As discussed in *Section 4.4*, these protonatable groups play a key role in the endosome escape of the complex, and so the cyclodextrin modification improves overall transfection. The testing of libraries of different variations of the chosen polymer is therefore required to find the most suitable chemical modifications for safe and effective RNA delivery.

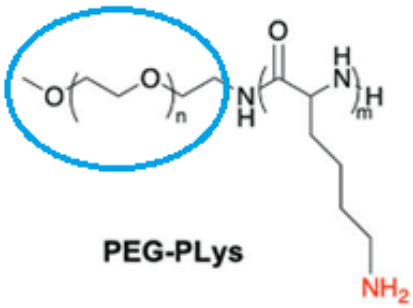

Figure. 5*. Example of the PEGylation modification (circled blue) to PLL* (Yang *et al.*, 2023).

Another class of anionic polymers used in PNP design are the PBAEs. These polymers are produced by the conjugation of amino monomers to diacrylates (Paunovska *et al.*, 2022). PBAEs, which feature biodegradable ester bonds (as depicted in *figure 3*) exhibit enhanced biodegradation and reduced cytotoxicity compared to PEI and PLL (Choi *et al.*, 2020). Also, formulating PBAEs with the addition of PEG increased their stability in serum and hence enabled the use of PBAE nanoparticles as safe and effective mRNA carriers in vivo (Kowalski *et al.*, 2019). To reveal how PBAE chemical structure impacts RNA delivery, libraries consisting of hundreds of distinct PBAEs were evaluated for their transfection efficacy in cell culture. This generated a design rulebook for successive PBAEs, suggesting the more effective polymers were typically hydrophobic, relatively smaller in size, contained either monoalcohol or dialcohol side groups and possessed linear amines (Anderson *et al.*, 2005). More broadly, studies like this emphasise the value of employing high-throughput chemical synthesis of nanoparticles, followed by high-throughput assessments of drug delivery efficacy (Paunovska *et al.*, 2022). Such approaches facilitate the identification of optimised variations of novel nanoparticle formulations.

One of the more recent advances using PBAE is its use in a PNP designed to deliver Cas13a mRNA in mice for the mitigation of influenza virus A infections. The translated Cas protein is responsible for initiating RNA cleavage against influenza RNA. Using a nebuliser, PNP-mRNA complexes were specifically targeted to the respiratory tract (Blanchard *et al.*, 2021).

3.3.2 Branched vs linear structures.

Once modified, polyplexes of the same chemical composition may then also differ in their dimensions, typically having either linear or branched configurations. It is key to identify the specific degree of branching that provides the best performance in transfection.

Previous studies have shown hyperbranched forms of PBAEs were favourable for mRNA delivery over linear structures (Wang *et al.*, 2016; A. K. Patel *et al.*, 2019). Branched forms of PEI (*figure 6*), PLL and other glycopolymers were all also more efficient at transfection when compared with their corresponding linear structures (Wang *et al.*, 2016). So, it is plausible that highly branched configurations of newly developed polymers could outperform the analogous linear form.

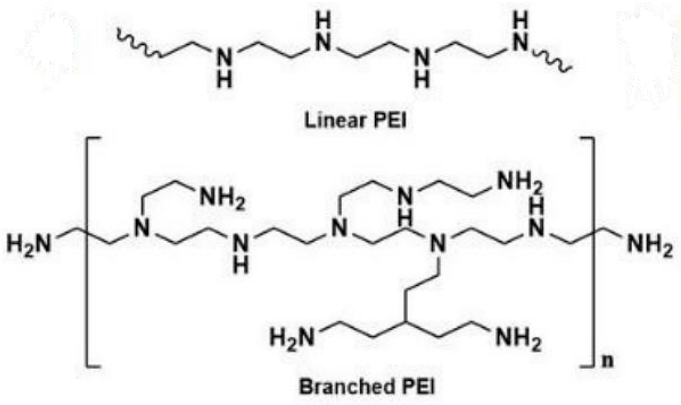

Figure. 6. *Structural comparison of linear and branched PEI* (Chen *et al.*, 2020).

As *figure 6* shows, branching PEI introduces secondary and tertiary amine groups, which will likely explain the differences in transfection observed (Chen *et al.*, 2020). Some researchers have also revealed how branched structures can interact with nucleic acids more strongly to significantly improve polyplex formation with nucleic acids compared to linear structures (Nakayama, 2012). This is ideal for generating relatively larger numbers of nanoparticles to optimise cellular uptake.

Furthermore, an additional benefit of using branched polymers is that their three-dimensional structure allows for the addition of multiple terminal functional groups compared to the limited two-dimensional structure of linear polymers. This makes them increasingly appealing for additional synthesis and optimisation (Zhao *et al.*, 2014).

3.3.3 Nitrogen-Phosphate ratio.

The nitrogen-phosphate (N/P) molar ratio is a measure of the positively charged amino groups ("nitrogen") from the polymer to negatively charged phosphate groups from the RNA. It is key to achieve the optimal N/P ratio for the specific formulation components. When the N/P ratio is too high, the increasing electrostatic interactions at play may restrain RNA release once inside the cell (Zhu *et al.*, 2018). Also an excess of cationic polymers could lead to unwanted cytotoxic effects (Aydin *et al.*, 2022). Or when the NP ratio is too low, all the RNA fails to completely complex (*figure 7*).

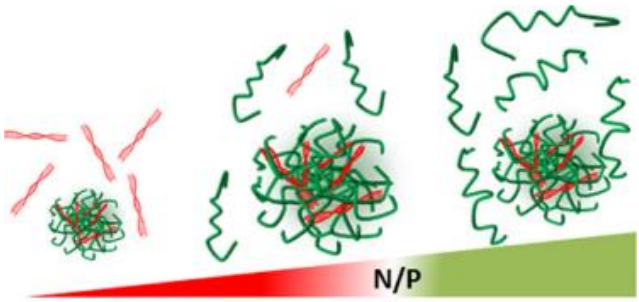

Figure. 7. *Formation of PNP-RNA complexes at varying N/P ratios: polymer (green) and RNA (red).*

Plus, alterations in N/P ratios cause differences to nanoparticle size, stability, and surface charge. Researchers have found that N/P ratios outside of the optimal can often lead to the formation of aggregates. This nanoparticle reorganisation may be a result of conformational changes in the polymers due to the increased ionic strength (Di Silvio *et al.*, 2019).

Differences in N/P ratios can greatly influence transfection efficacy and toxicity levels; therefore, it is vital to optimise N/P ratio in formulation steps.

4. Nanoparticle internalisation within the cell

The mechanisms of cellular internalisation, intracellular trafficking and endosomal escape are speculated greatly for different RNA-delivery systems. This even applies for the more-studied LNPs. Uncovering how nanoparticle size, shape and chemical composition affects the various stages of cellular internalisation is the aim for future research.

The lack of understanding surrounding the detailed mechanism and route that RNA takes inside the cell to the translational machinery is considered the limiting factor in improving the efficacy of the

nanoparticles for therapeutics. Importantly, the successful endocytosis of PNP-RNA complexes does not automatically result in translation (Wu and Li, 2021). When designing delivery systems, the greatest challenge is the ability of nanoparticles to target the correct cells, then once endocytosed, also allow the RNA to escape its vehicle and cross the endosomal membrane. Failing to combine effective endosome escape with successful nanoparticle uptake demands higher dosage, increasing the risk of toxicity (Paramasivam *et al.*, 2021).

Despite extensive research in identifying efficient delivery systems, the results are limited and conflicting about their internalisation mechanisms. To highlight potential routes for PNP delivery of RNA, research on LNPs is considered in this chapter also. However, when comparing PNPs with LNPs, it is important to recognise that the mechanisms they employ for endosome escape primarily different. Cationic polymers typically lack the highly hydrophobic domain of LNPs, and so cannot interact and fuse with the endosomal membrane directly, as in the case for cationic lipids (Tros de Ilarduya, Sun and Düzgüneş, 2010). This is why some scientists engineer hydrophobic moieties into cationic polymers to further improve their efficiency, despite the consequential implications for loading genetic material (Solomun *et al.*, 2021).

4.1 Cell Targetability

Although targeting specific cells is less of a priority for mRNA vaccines, it is essential for other RNA therapies. Targeting nanoparticles to the specific cell required for transfection should hypothetically increase transfection efficiency whilst also reducing off-target side effects. Tuning formulation factors for this directivity may include varying polymer composition, particle size, surface charge and the degree of PEGylation (Cabral *et al.*, 2018).

To further increase targetability of desired cells, surface modifications with a specific ligand would result in more precise and rapid uptake via the receptor-mediated mechanisms (Wu and Li, 2021). Research has shown PLL can be easily functionalised with the ligands, folic acid, glucose, galactose and CAFW (Cys-Ala-Gly-Trp) peptide). Specifically, folate-coated PEG-PLL complexed with nucleic acids demonstrated higher transfection activity than its nontargeting equivalent in cells expressing folate receptors (Dai *et al.*, 2011). The circulation half-life was improved by additionally coating the PLL polyplexes with PEG, as binding to plasma proteins was prevented (Zheng *et al.*, 2021).

Therefore, improving cell targetability of polyplexes is highly desirable and provides future perspectives for RNA delivery by PNPs.

4.2 Cellular uptake

To enter the cell, the nanoparticle must be endocytosed via one or more mechanism; typically, the clathrin-mediated, caveolin-mediated or independent pathways (*figure 8*) (Mitchell *et al.*, 2020). Often, more than one mechanism is activated. Numerous cell surface proteins facilitate endocytosis such as clathrin, flotillin, RhoA, amongst others. As with the other cellular internalisation steps leading to transfection, it is the nanoparticle physiochemical properties and size that are responsible for defining the exact cellular uptake mechanism (Sahay, Alakhova and Kabanov, 2010). The addition of formulation components like cholesterol or PEG lipids can promote membrane fusion if required for uptake (Cheng and Lee, 2016). Or, size helps determine mechanism, e.g. nanoparticles approximately 60 nm in size will use caveolin-mediated pathway, whereas nanoparticles approximately 100 nm in size utilise the clathrin-mediated pathway (Rennick, Johnston and Parton, 2022). It remains unknown how the uptake mechanism may ultimately impact PNP fate within a cell.

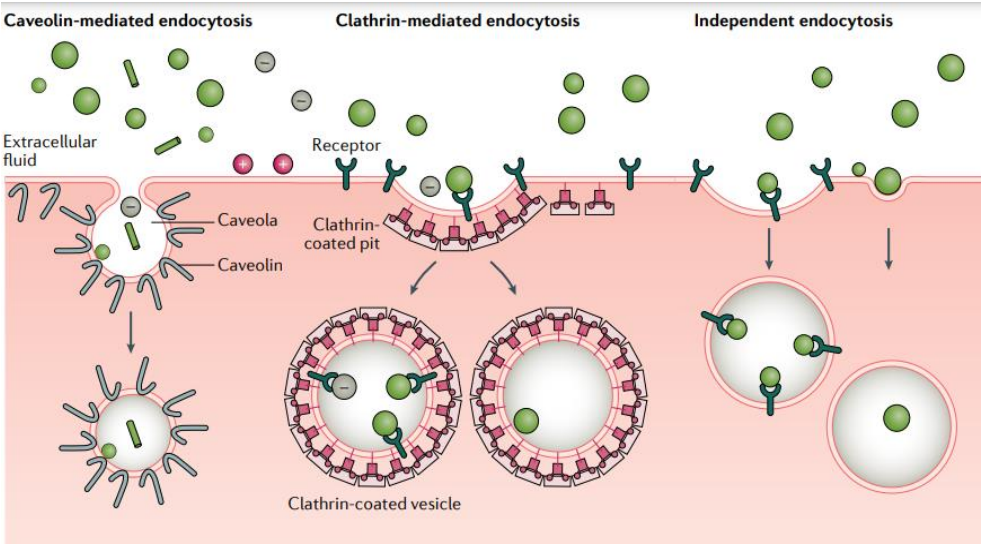

Figure. 8. *Common uptake pathways for PNPs within a cell: internalisation of PNPs can occur via non-specific or specific interactions, contingent upon their size, surface properties and charge* (Mitchell *et al.*, 2020).

After successful endocytosis, regardless of their route of entry, the nanoparticles are compartmentalised inside the cell within membrane-bound vesicles, called endosomes (Sahay, Alakhova and Kabanov, 2010). To measure the uptake of polyplexes, the complexed mRNA can be labelled with a fluorescent dye such as a Cy5 or DY547 label. After an hour, the nanoparticles should have been internalised and it is possible to observe the mean fluoresence intensity in the cells (Jiang *et al.*, 2020). *Figure 9* demonstrates how this nanoparticle internalisation is visualised using confocal

microscopy. The images reveal how HeLa cells uptake most of the DY547-labelled LNP-siRNA during the first 6 hours (Du Rietz *et al.*, 2020).

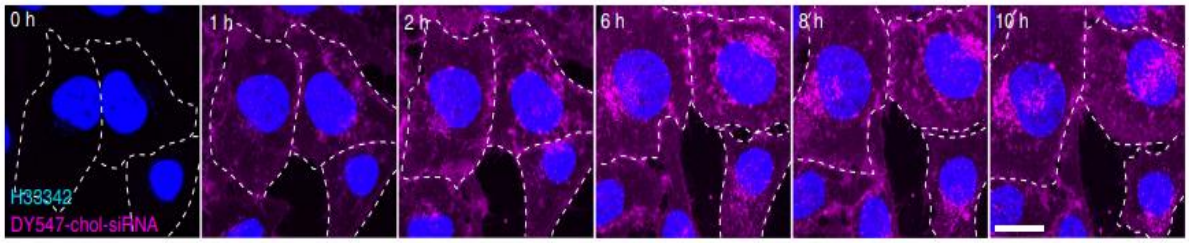

Figure. 9. *Uptake of LNP-siRNA (pink) uptake monitored for 10 hours in HeLa cells (outlined) using confocal microscopy. Scale bar = 20 µm* (Du Rietz *et al.*, 2020).

4.3 Cellular trafficking

The endosomal recycling pathway is responsible for trafficking extracellular contents to various locations within the cell. Like all internalised cargo, the engulfed nanoparticles collect into an early endosome which constitutes several small vesicles and tubules. This early endosome is slightly acidic (pH 6.0-6.8) (O'sullivan and Lindsay, 2020).

The nanoparticles then have two options. Ideally, they should exit the endosome during its early or late stage (pH drops to 5.5 (Tros de Ilarduya, Sun and Düzgüneş, 2010).). Otherwise, the nanoparticles would be at risk of degradation after organisation into lysosomes (pH 4.5-5.0) (O'sullivan and Lindsay, 2020). The latter is the case for the majority of the successfully delivered material, as endosome escape efficiency is far from maximum (Sahay, Alakhova and Kabanov, 2010; Sahay *et al.*, 2013).

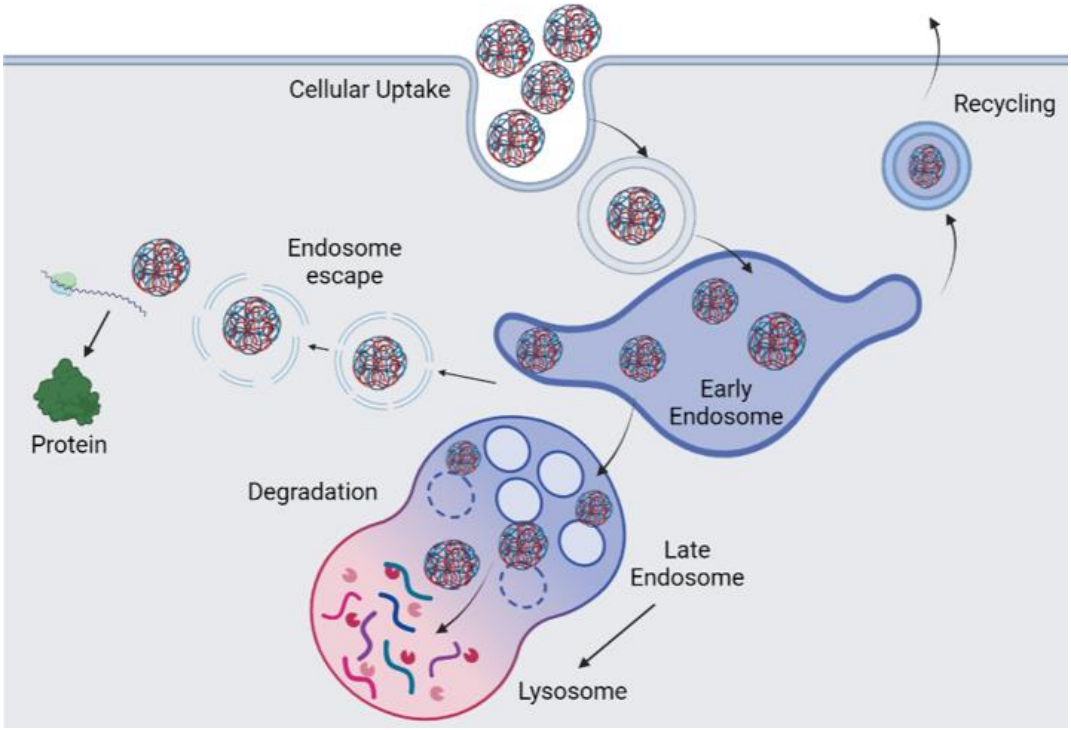

Figure. 10. *Overview of endosomal recycling pathway showing PNP-mRNA endocytosis converging at the early endosome, where it is sorted for either escape or onward transport (degradation or recycling). BioRender adaptation of figure taken from* (O'sullivan and Lindsay, 2020).

In a study using LNPs, Patel *et al.* (2017) examined nanoparticle trafficking from early endosome to lysosome. Their results revealed how late endosome/lysosome formation is essential for functional delivery of mRNA. This is because a signalling complex resides on the lysosomal surface which is involved in modulating mRNA translation. Enhancing this pathway pharmacologically increased LNP-mediated mRNA delivery, revealing the pathways role (Patel *et al.*, 2017).

However, this research is contradictory to other findings. Another study used specific fluorescent dyes for early, late endosome and RNA to show cellular colocalization. The images testified that escape is constrained to an early endosomal compartment and terminated upon conversion to a late endosome. Paramasivam *et al*. also found that this release of LNP-RNA occurred over a very narrow (approximately 10 minutes) time window (Paramasivam *et al.*, 2021). Gilleron *et al.* had previously identified similar, indicating endosomal escape occurs during a limited period of time when LNPs reside in a specific compartment that shares early and late endosomal characteristics, long before conversion to a lysosome (Gilleron *et al.*, 2013).

These differences in observations may possibly highlight variability in nanoparticle trafficking amongst various cell types. Also, it could reflect how various particle properties, e.g., different pH sensitivities impact cellular trafficking.

For PNPs, even less is understood about the stage of endo-lysosomal maturation in which RNA escapes into the cytosol. It is probable that polyplex composition and structure influences the exact mechanism (Wu and Li, 2021). Therefore, further research is required to identify the overall relationship between different nanoparticle properties, how they are trafficked in the cell and the resulting impact on transfection efficiency. This will provide insights for the development of more effective and safer delivery strategies.

To achieve this, it is vital that the distribution of PNP-mRNA complexes in endosomal compartments is visualised. The current available imaging methods include fluorescently labelling or immunostaining endosomes. For example, immunostains EEA1 and APPL1 label various early endosomes whilst LAMP1 reveals late endosomes. Then by labelling the RNA or PNP, the proportion of co-localisation across cellular compartments can be quantified (Gilleron *et al.*, 2013).

Fundamentally, whatever the trafficking mechanism, it is key that efficient and nontoxic PNPs carry RNA to the necessary compartments for effective release whilst not interfering with endosomal function (Paramasivam *et al.*, 2021).

Additionally, the complexity of the endosomal network, its intricate trafficking machinery and dynamic process must not be underestimated. This plays an important role in dynamically exchanging cargo between organelles, constantly changing in size and position over time. Consequently, a detailed, quantitative and high-resolution analysis is required to interpret the precise interaction between nanoparticles and the endosomal network (Paramasivam *et al.*, 2021).

4.4 Endosome escape

Endosome entrapment of the nanoparticles and failure of RNA escape from the vesicle limits the cellular bioavailability of mRNA and subsequent protein expression. Plus, nanoparticles must evade barriers including exocytosis, trafficking to other organelles or lysosomal degradation. Hence, endosome escape is the next fundamental step in delivering mRNA to ribosomes (Wu and Li, 2021).

Irrespective of the specific release mechanism, imaging studies have demonstrated that administered nucleic acids are predominantly sequestered within endosomes. Consequently, they undergo degradation in the lysosome, with only a small portion being successfully released to the cytosol (Suh *et al.*, 2012; Sahay *et al.*, 2013). To provide to a quantitative perspective, an investigation regarding the delivery of small interfering RNA (siRNA) revealed that less than 2% of the provided LNPs-siRNA managed to escape from the endosome and reach the cytosol (Maugeri *et al.*, 2019). This implies that there are opportunities to enhance transfection efficiency via the endosomal escape pathways.

As such a small percentage of the delivered mRNA typically reaches the cytosol, traditional microscopy techniques are far from ideal for exposing endosomal escape sites and mechanisms due to sensitivity limitations (Patel *et al.*, 2017). Reliable and sensitive methods for the quantification of endosomal escape have yet to be identified and developed, owing to the lack of experimental data. Current methods of detection include fluorescent labelling assays, leakage assays, membrane lysis assays and transfection assays – each of which have significant limitations. Recently, Jiang *et. al* (2020) developed a novel protein probe that aims to quantify the cytosolic entry of exogenous material. A deactivated form of the Renilla luciferase (ddRLuc) probe can be simultaneously encapsulated with mRNA in the same delivery nanoparticle. Only then after endosome escape and entry into the cytosol can the activity of the protein probe be restored via its interaction with a cytosolic enzyme, generating an RLuc signal (Jiang *et al.*, 2020). Accurately quantifying endosome escape is the first step in uncovering the exact mechanisms at play.

The most supported mechanism for polymer-based endosomal escape is the rupturing of endosomes caused by the 'proton sponge effect'. Other mechanisms have been suggested for LNPs including the lipoplex fusion with the endosomal membrane or pH-triggered nanoparticle destabilisation (Wu and Li, 2021), amongst others. It is likely that different nanoparticle structures, with varying compositions and surface properties, exploit different pathways, with possibly even a combination of mechanisms at play.

It also remains misunderstood whether the nanoparticle-RNA complex or just the isolated, naked RNA escapes the endosome. It is likely that it varies depending on the mechanism at play. For example, with LNP fusion with endosomal membranes, it appears the RNA is isolated and released in unison (Li, Zhang and Dong, 2019).

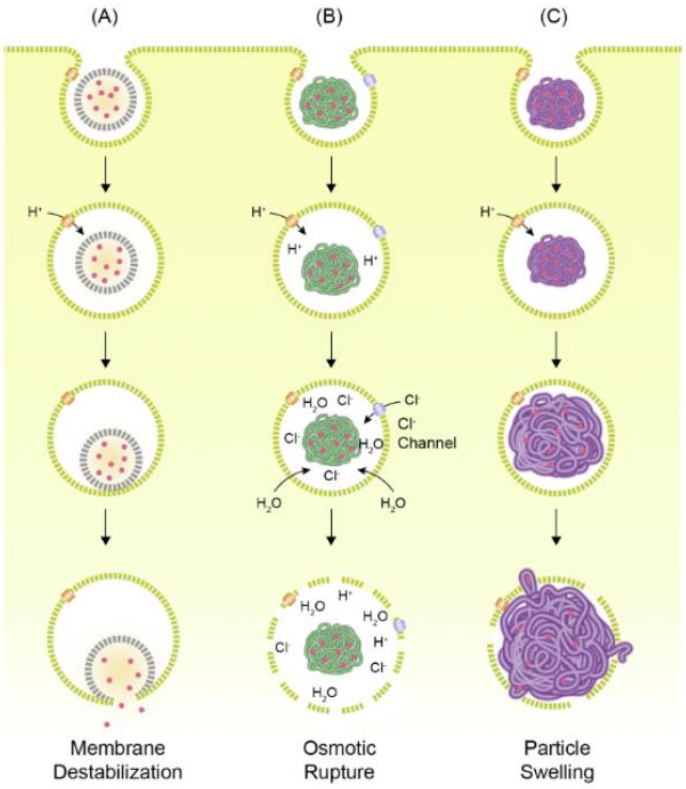

Figure. 11. *Potential endosomal escape mechanisms of nanoparticles that have received the most evidence, currently. A) Fusion of nanoparticles with the endosomal membrane can create pores in the endosome. B) Protonatable nanoparticles cause proton influx, increasing endosome osmotic pressure. C) Nanoparticles may swell in acidic environment due to charge-charge interactions potentially causing endosomes to burst. Figure from* (Patel *et al.*, 2019).

4.4.1 The "proton sponge" effect.

The favoured mechanism for PNP escape from endosomes is facilitated through the 'proton sponge effect'. This described phenomenon is enabled by cationic polyplexes containing protonatable groups providing them with a high buffer capacity. The polymers can then bind the protons that are actively transported into the endosomal lumen by membrane-bound pumps as the endosome matures. Thereby, the binding of protons by polymers slows endosomal acidification (Wu and Li, 2021).

Consequently, to compensate, it is suggested that the proton pumps will translocate additional protons into the endosome compartment to achieve the required lower pH for the endosome recycling pathway. To neutralise this charge, chloride ions also enter the endosome resulting in an increased ionic concentration. This leads to the increased diffusion of water to maintain osmolarity causing an increase in osmotic pressure and therefore, endosome swelling (*figure 11B)*.

Another understanding of this phenomenon describes how it is the polymer itself that swells owing to inter-charge repulsion between protonated amines (Patel *et al.*, 2019). This may cause breakages in the endosome membrane (*figure 11C*) independent of osmotic pressure. Either as individual

mechanisms or a combination, these swelling events are hypothesised to cause adequate endosomal damage for the release of nucleic acids in the cytosol (Vermeulen *et al.*, 2018).

Conclusive evidence for this hypothesis remains vague. Some supporting evidence found that endosomal acidification slows downs upon cell administration of buffering polymers compared to endosomes with non-buffering polymers that became increasingly acidic more rapidly (Akinc *et al.*, 2005). Also, others reported relationships between endosome size and leakiness with endosome escape efficiency. As would be expected with the proton sponge mechanism, smaller endosomes increased escape activity and more leaky membranes reduced endosome rupture events. This was identified by comparing escape between different cell types: HeLa cells with small endosomes, A549 with larger endosomes and H1299 with leaky endosomes (Vermeulen *et al.*, 2018).

However, is it unclear whether the observed differences are only due to variations in endosomal properties or represent the other countless factors that differ amongst cell type. Therefore, to validate these theories, a method that increases endosomal size within the same cell type is required (Patel *et al.*, 2019).

PEI is the main accepted example to utilise the photon sponge method for facilitating endosomal damage. By further modifying PEI with histidine moieties (pKa ~6.0), the buffer capacity is increased, leading to more polymer protonation and increased endosomal osmotic pressure, whilst also lowering cytotoxicity compared to unmodified PEI (Bertrand *et al.*, 2011; Démoulins *et al.*, 2016). Therefore, in theory, all cationic polymers that contain protonatable secondary and/or tertiary amine groups with a pKa near to late endosome pH should exhibit effective transfection due to the proton sponge phenomenon (Vermeulen *et al.*, 2018). For some polymers (e.g. PEI shown in *figure 6*), branched variations will contain more secondary amines and tertiary amines.

However, others argue that this retardation of endosome maturation and cargo degradation may only exacerbate low transfection rates. Slowing down the endosome recycling pathway likely prevents regular, cellular homeostasis and lysosomal degradation of accumulated nanoparticles, contributing to cytotoxic effects and thereby reducing transfection capacity (Paramasivam *et al.*, 2021).

Visualising endosome escape and the 'proton sponge' phenomenon

Advances in imaging techniques (e.g. electron microscopy and confocal laser scanning microscopy) and omics-based approaches (Patel *et al.*, 2019) should allow scientists to better investigate the endosome escape mechanisms for various nanoparticles. This should, in turn, improve the innovation of advanced nanoparticle formulations and their rational design for the most effective transfection (Zhu *et al.*, 2022).

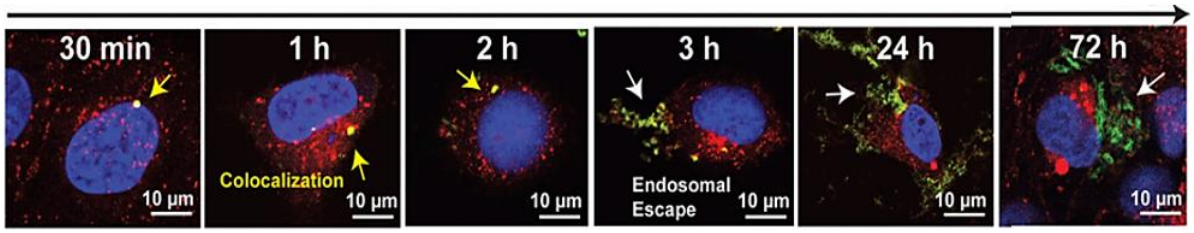

Figure. 12. *Time-dependent endosomal escape: Confocal laser-scanning microscopy images demonstrate release of 'nanopieces' (based on DNA-inspired Janus base nanotubes) complexed with siRNA from late endosomes in C28/I2 cells (human chondrocyte cell line). Fluorescently labelled siRNA (green), nuclei (blue), late endosomes (red), colocalization between siRNA and endosomes (yellow).* (Lee *et al.*, 2021)

Currently, live imaging has revealed the time-dependent endosomal escape of nanoparticles. Lysotracker-Red was used to visualise late endosomes directly, whilst the nanoparticle-siRNA complexes where fluorescently labelled green (Lee *et al.*, 2021). The images reveal how, after endocytosis, there is a co-localisation between nanoparticles and endosomes before their eventual release (*figure 12*).

Another study, using linear PEI nanoparticles to delivery nucleic acids into HeLa cells, visualised the endosome "burst" in real time (*figure* 13). The small polyplex is bursts opens and its fluorescently labelled nucleic acid contents are rapidly released into the cytosol (Rehman, Hoekstra and Zuhorn, 2013).

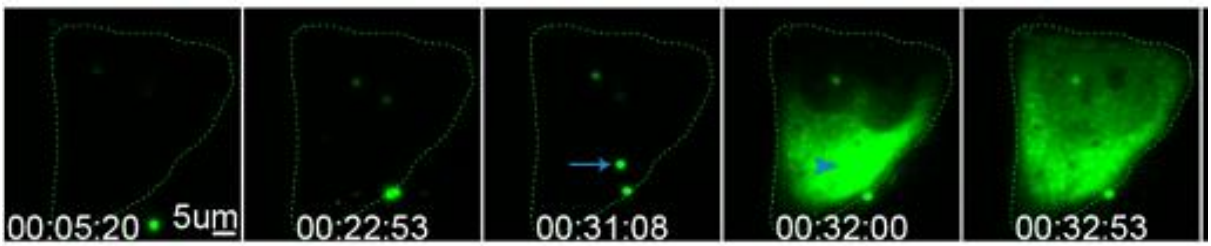

Figure. 13*. Live cell imaging of PEI uptake (arrow) and endosomal burst of nucleic acid (green) within HeLa cells (panel 4-5)* (Rehman, Hoekstra and Zuhorn, 2013).

Figure 14 shows potential visual evidence for the proton sponge mechanism as inhibiting the acidification of endosomes, and thereby endosome progression, prevents nanoparticle release (Kichler *et al.*, 2001). The nanoparticles used in this are considered to have a buffering capacity comparable to that of PEI and PLL, hence why the proton sponge mechanism is assumed (Lee *et al.*, 2021). This study strongly confirms the key role endosome progression has in escape but, further evidence is required to prove this endosome acidification-dependent release is acting via the proton sponge phenomenon.

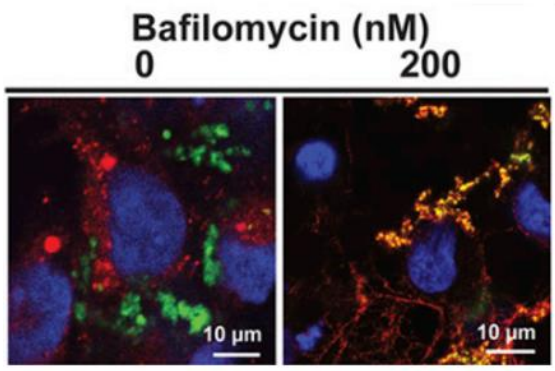

Figure. 14. *Inhibition of the proton sponge effect: Confocal laser-scanning microscopy images show significant reduction in nanoparticle (green) escape from endosomes (red) when C28/I2 treated with endosomal acidification inhibitors (bafilomycin A1).* (Lee *et al.*, 2021).

Fundamentally, however, this visualisation of endosome escape can be tailored credibly to the investigation of other delivery systems, including polymers in various other cell lines.

4.4.2 Alternative endosome escape mechanisms for PNPs

Alternative explanations for PNP endosome escape suggest that PEI and other cationic polymers create individual pores in endosomal membranes that allow nucleic acid cargo to escape (Choudhury, Kumar and Roy, 2013). Computational simulations have demonstrated that the cationic polymer chain could interfere with the stability of the lipid bilayer of the endosomal membrane (Mecke *et al.*, 2005) and cause membrane permeability (Hong *et al.*, 2006). The model suggests that hydrophillic pores are formed, penetrating across the membrane (Bus, Traeger and Schubert, 2018). This alternate theory is supported by the argument that cationic polymers do not influence endosome maturation, opposing the basis of the proton sponge mechanism (Benjaminsen *et al.*, 2013). Hence, why there is uncertainty regarding the dominant mechanism for PNP-RNA escape.

4.4.3 Endosome escape mechanisms associated with LNPs.

Endosomal membrane fusion

In contrast to the uncertainty around endosomal escape mechanisms for PNPs, it is accepted that LNPs typically fuse with the endosomal membrane to facilitate escape (*figure 11A)*. Administered cationic lipids trigger the cytosolic-facing anionic lipids of the membrane bilayer to flip and instead complex via electrostatic interactions with the cationic lipids (Miao et al., 2020). Bound together, they form an inverted hexagonal structure, displacing the nucleic acid cargo and enabling its release. Researchers have found that the formation of this structure is promoted by incorporating a helped lipid, such as DOPE or DSPC (*figure 2*), into the nanoparticle formulation, leading to an increased transfection efficiency (Xu, Saltzman and Piotrowski-Daspit, 2021). Optimising the types, ratios and physiochemical properties of the ionisable lipids of the LNP can increase membrane fusion and thereby endosomal escape, also (Hou *et al.*, 2021).

Therefore it could be considered that cationic polymers with hydrophobic regions may act similarly to cationic lipids and interact with the negatively charged endosomal membrane lipids to destabilise the bilayer (Kowalski *et al.*, 2019; Li, Zhang and Dong, 2019). However, this mechanism has failed to receive compelling experimental support for PNPs and is likely restricted to lipoplexes. Nevertheless, the hypothesis has initiated the investigation into altering PNP formulations with the addition of multi-tailed, ionisable zwitterionic phospholipids to generate polymer-lipid hybrid nanoparticles (Meng and Grimm, 2021). It has been found that the integration of hydrophobic segments into polyplex structures helps lower their charge density, leading to more efficient nucleic acid release and transfection (Zheng *et al.*, 2021).

However, this mechanism contradicts how the complexation of cationic lipids with negatively charged RNA should be favoured more than dissociation in the acidic lumen of the endosome (Wu and Li, 2021).

Novel theories

Some newer mechanisms have also been theorised, sharing similarities with those mentioned previously. They offer unique perspectives to understanding the method of endosome escape.

Using high-resolution microscopy, Paramasivam *et al.* imaged the co-localisation of LNP-mRNA complexes with sub-endosomal compartments. The nanoparticles appeared to escape from narrow regions of the endosome otherwise known as endosomal recycling tubules. The research proposed that mRNA escape events were most prominent in endosomes possessing these recycling tubules (Paramasivam *et al.*, 2021).

Other ideas include the role of transporter proteins located within endosomal membranes that modulate the digestion and recycling of material. For example, Niemann-Pick type C1 (NPC1) is known for its key regulatory role in the movement of lipids within cells and specifically, across membranes. When administrated with LNP-RNA complexes, NPC1-deficient cells retained more LNPs inside late endosomes and lysosomes, resulting in less nucleic acid activity (Sahay *et al.*, 2013).

Finally, nanoparticle structures that are pH responsive may experience conformational changes caused by protonation or bond cleavage. For example, the acidic environment could favour the hydrolysis of certain labile bonds within the polymer (Kanamala *et al.*, 2016). Or, pH-sensitive endosomal proteins may become ionised and thereby activated to catalyse polymer degradation (Jiang *et al.*, 2020). Both would theoretically lead to nanoparticle dissociation and potentially supporting its escape from the endosome.

This research should assist in generating novel hypotheses to explain the method for endosomal escape of PNP-delivered RNA. The variations on the literature likely reflect the differences between cell lines that have been recognised for RNA delivery. Such variations include nanoparticle internalisation rates, endosomal pH, size and recycling rates and transfection rates. Therefore, all *in vitro* data should be considered with caution as accurate extrapolation to function *in vivo* cannot be assumed automatically. Nanoparticles should be designed for their specific target tissues, as endosomal escape is specific to both nanoparticle composition and cell-type (Xu, Saltzman and Piotrowski-Daspit, 2021).

4.5 Translation

It is assumed that after escaping the endosome, the mRNA is readily accessible to the translation machinery in the cytosol. This is supported quantitatively by data showing a strong correlation between rate of endosome escape and transfection. Therefore, it is probable that once escaped, the nanoparticle and mRNA are separated. At least, the binding of the nanoparticle does not impede mRNA translation. Some researchers suggest that separation of mRNA from the polymer occurs before endosomal escape and therefore is immediately translatable upon reaching the cytosol. This was shown for (poly(amine-*co*-ester) (PACE) (Jiang *et al.*, 2020). As with the other stages of RNA delivery, this too remains inconclusive.

5. Future perspectives

With a better insight *in vitro*, the future of PNP research should look to compare how these theories, tested in cell culture, apply *in vivo*. It is key that any extracellular factors with the potential for modulating nanoparticle characteristics or trafficking are identified and considered. There is a risk of unforeseen off-target effects arising from alterations in particle size, surface charge, or aggregation in the blood (Yang *et al.*, 2023). Therefore, there is a strong need to develop pertinent *in vitro* models that can accurately predict the *in vivo* behaviour of novel PNP-mRNA complexes.

Furthermore, personalising and modifying RNA therapy for individual patients by optimising delivery vehicles provides a potential future for nanoparticle design. The application of specific ligands to PNPs can enable targeted delivery to specific cells (Barbier *et al.*, 2022). It is essential to optimise ligand requirements including density and binding affinity, according to the specific therapeutic circumstance.

6. Conclusion

To conclude, PNPs offer a promising ability as delivery vehicles for various RNA therapeutics. However, several important key questions and areas for further development remain. Enhancing mRNA transfection efficiency, improving tissue targetability and ensuring patient compliance are key focus areas. As knowledge improves, applications will extend beyond mRNA vaccines to novel therapeutics that, for example, facilitate protein replacement in specific cells.

Crucially, future work is required to improve the understanding of the relationship between PNP formulation characteristics and uptake and trafficking mechanisms. By uncovering the determining factors within nanoparticle variations that influence their efficiency, researchers can design optimal supramolecular nanoparticle formulations and ultimately realise the maximum potential of RNA medicines. Specifically, as mentioned previously, the bottleneck of transfection efficiency for existing PNPs is the challenge of endosome escape. Hence, the discovery and development of new nanoparticle modifications that enhance endosome escape capacity would be a significant step towards improving overall efficacy and safety.

During the testing of novel PNP designs, it is crucial to confirm whether endosome escape is the internalisation step that primarily restricts transfection efficiency, and which mechanism the polymer utilises. As the specific PNP, RNA cargo and cell-type all impact transfection efficiency, it is key to

identify mechanisms for each unique combination. This objective necessitates a multidisciplinary and collective approach involving research biologists and formulation scientists.

Acknowledgments

I am extremely grateful to Professor Cameron Alexander and Dr Sal Jones from the School of Pharmacy at the University of Nottingham, for their invaluable assistance, guidance, and feedback.

Also special thanks to Professor Stephen Harding, the Head of the National Centre for Macromolecular Hydrodynamics (NCMH) at the University of Nottingham, for all his help organising the Industrial Project Module (BIOS4152) and my peers on the MRes Biomolecular Technology course for their moral support.

References

Akinc, A. *et al.* (2005) 'Exploring polyethylenimine-mediated DNA transfection and the proton sponge hypothesis', *The journal of gene medicine*, 7(5), pp. 657–663. doi: 10.1002/JGM.696.

Anderson, D. G. *et al.* (2005) 'Structure/property studies of polymeric gene delivery using a library of poly(β-amino esters)', *Molecular Therapy*, 11(3), pp. 426–434. doi: 10.1016/j.ymthe.2004.11.015.

Aydin, O. *et al.* (2022) 'Determination of Optimum Ratio of Cationic Polymers and Small Interfering RNA with Agarose Gel Retardation Assay', *Methods in Molecular Biology*, 2434, pp. 117–128. doi: 10.1007/978-1-0716-2010-6_7.

Barbier, A. J. *et al.* (2022) 'The clinical progress of mRNA vaccines and immunotherapies', *Nature Biotechnology*, 40(6), pp. 840–854. doi: 10.1038/s41587-022-01294-2.

Benjaminsen, R. V. *et al.* (2013) 'The Possible "Proton Sponge " Effect of Polyethylenimine (PEI) Does Not Include Change in Lysosomal pH', *Molecular Therapy*, 21(1), pp. 149–157. doi: 10.1038/MT.2012.185.

Bertrand, E. *et al.* (2011) 'Histidinylated linear PEI: a new efficient non-toxic polymer for gene transfer', *Chemical Communications*, 47, pp. 12547–12549. doi: 10.1039/c1cc15716g.

Blanchard, E. L. *et al.* (2021) 'Treatment of influenza and SARS-CoV-2 infections via mRNA-encoded Cas13a in rodents', *Nature Biotechnology*, 39(6), pp. 717–726. doi: 10.1038/s41587-021-00822-w.

Brader, M. L. *et al.* (2021) 'Encapsulation state of messenger RNA inside lipid nanoparticles', *Biophysical Journal*, 120(14), pp. 2766–2770. doi: 10.1016/J.BPJ.2021.03.012.

Bus, T., Traeger, A. and Schubert, U. S. (2018) 'The great escape: how cationic polyplexes overcome the endosomal barrier', *Journal of Materials Chemistry B*, 6(43), pp. 6904–6918. doi: 10.1039/C8TB00967H.

Cabral, H. *et al.* (2018) 'Block Copolymer Micelles in Nanomedicine Applications', *Chemical reviews*, 118(14), pp. 6844–6892. doi: 10.1021/ACS.CHEMREV.8B00199.

Chen, Z. *et al.* (2020) 'Recent advancements in polyethyleneimine-based materials and their biomedical, biotechnology, and biomaterial applications', *Journal of Materials Chemistry B*, 8(15), pp. 2951–2973. doi: 10.1039/C9TB02271F.

Cheng, X. and Lee, R. J. (2016) 'The role of helper lipids in lipid nanoparticles (LNPs) designed for oligonucleotide delivery', *Advanced Drug Delivery Reviews*, 99, pp. 129–137. doi: 10.1016/J.ADDR.2016.01.022.

Choi, J. *et al.* (2020) 'Nonviral polymeric nanoparticles for gene therapy in pediatric CNS malignancies', *Nanomedicine: Nanotechnology, Biology, and Medicine*, 23. doi: 10.1016/J.NANO.2019.102115.

Choi, Y. H. and Han, H.-K. (2018) 'Nanomedicines: current status and future perspectives in aspect of drug delivery and pharmacokinetics', *Journal of Pharmaceutical Investigation*, 48, pp. 43–60. doi: 10.1007/s40005-017-0370-4.

Choudhury, C. K., Kumar, A. and Roy, S. (2013) 'Characterization of conformation and interaction of gene delivery vector polyethylenimine with phospholipid bilayer at different protonation state', *Biomacromolecules*, 14(10), pp. 3759–3768. doi: 10.1021/BM4011408/SUPPL_FILE/BM4011408_SI_001.PDF.

Dai, J. *et al.* (2011) 'Polyethylenimine-grafted copolymer of poly(l-lysine) and poly(ethylene glycol)

for gene delivery', *Biomaterials*, 32(6), pp. 1694–1705. doi: 10.1016/J.BIOMATERIALS.2010.10.044.

Démoulins, T. *et al.* (2016) 'Polyethylenimine-based polyplex delivery of self-replicating RNA vaccines', *Nanomedicine: Nanotechnology, Biology and Medicine*, 12(3), pp. 711–722. doi: 10.1016/J.NANO.2015.11.001.

Deverman, B. E. *et al.* (2018) 'Gene therapy for neurological disorders: progress and prospects', *Nature Reviews Drug Discovery*, 17(9), pp. 641–659. doi: 10.1038/nrd.2018.110.

Dowdy, S. F. (2017) 'Overcoming cellular barriers for RNA therapeutics', *Nature Biotechnology*, 35(3), pp. 222–229. doi: 10.1038/nbt.3802.

Duncan, R., Ringsdorf, H. and Satchi-Fainaro, R. (2006) 'Polymer therapeutics: Polymers as drugs, drug and protein conjugates and gene delivery systems: Past, present and future opportunities', *Advances in Polymer Science*, 192(1), pp. 1–8. doi: 10.1007/12_037/COVER.

Finn, J. D. *et al.* (2018) 'A Single Administration of CRISPR/Cas9 Lipid Nanoparticles Achieves Robust and Persistent In Vivo Genome Editing', *Cell reports*, 22(9), pp. 2227–2235. doi: 10.1016/J.CELREP.2018.02.014.

Gilleron, J. *et al.* (2013) 'Image-based analysis of lipid nanoparticle-mediated siRNA delivery, intracellular trafficking and endosomal escape', *Nature Biotechnology*, 31(7), pp. 638–646. doi: 10.1038/nbt.2612.

Gindy, M. E. *et al.* (2014) 'Mechanism of Macromolecular Structure Evolution in Self-Assembled Lipid Nanoparticles for siRNA Delivery', *Langmuir*, 30(16), pp. 4613–4622. doi: 10.1021/la500630h.

Han, X. *et al.* (2021) 'An ionizable lipid toolbox for RNA delivery', *Nature Communications*, 12(1), pp. 1–6. doi: 10.1038/s41467-021-27493-0.

Herndon, M. K., Quirk, C. C. and Nilson, J. H. (2016) 'Control of Hormone Gene Expression', *Endocrinology: Adult and Pediatric*, 2, pp. 16–29. doi: 10.1016/B978-0-323-18907-1.00002-0.

Hong, S. *et al.* (2006) 'Interaction of Polycationic Polymers with Supported Lipid Bilayers and Cells: Nanoscale Hole Formation and Enhanced Membrane Permeability', *Bioconjugate Chemistry*, 17(3), pp. 728–734. doi: 10.1021/bc060077y.

Hou, X. *et al.* (2021) 'Lipid nanoparticles for mRNA delivery', *Nature Reviews Materials*, 6, pp. 1078–1094. doi: 10.1038/s41578-021-00358-0.

Huang, L. *et al.* (2022) 'Advances in Development of mRNA-Based Therapeutics', *Current Topics in Microbiology and Immunology*, 440, pp. 147–166. doi: 10.1007/82_2020_222/COVER.

Jiang, Y. *et al.* (2020) 'Quantitating Endosomal Escape of a Library of Polymers for mRNA Delivery', *Nano letters*, 20, pp. 1117–1123. doi: 10.1021/acs.nanolett.9b04426.

Kamaly, N. *et al.* (2016) 'Degradable Controlled-Release Polymers and Polymeric Nanoparticles: Mechanisms of Controlling Drug Release', *Chemical reviews*, 116(4), pp. 2602–2663. doi: 10.1021/ACS.CHEMREV.5B00346.

Kanamala, M. *et al.* (2016) 'Mechanisms and biomaterials in pH-responsive tumour targeted drug delivery: A review', *Biomaterials*, 85, pp. 152–167. doi: 10.1016/J.BIOMATERIALS.2016.01.061.

Ke, X. *et al.* (2020) 'Surface-Functionalized PEGylated Nanoparticles Deliver Messenger RNA to Pulmonary Immune Cells', *ACS applied materials & interfaces*, 12(32), p. 35835. doi: 10.1021/ACSAMI.0C08268.

Kichler, A. *et al.* (2001) 'Polyethylenimine-mediated gene delivery: a mechanistic study', *The journal*

of gene medicine, 3(2), pp. 135–144. doi: 10.1002/JGM.173.

Kowalski, P. S. *et al.* (2019) 'Delivering the Messenger: Advances in Technologies for Therapeutic mRNA Delivery', *Molecular Therapy*, 27(4), pp. 710–728. doi: 10.1016/J.YMTHE.2019.02.012.

Lee, J. *et al.* (2021) 'DNA-inspired nanomaterials for enhanced endosomal escape', *Proceedings of the National Academy of Sciences of the United States of America*, 118(19), p. e2104511118. doi: 10.1073/PNAS.2104511118/SUPPL_FILE/PNAS.2104511118.SM01.MP4.

Li, B. *et al.* (2023) 'Combinatorial design of nanoparticles for pulmonary mRNA delivery and genome editing', *Nature biotechnology*, pp. 1–6. doi: 10.1038/s41587-023-01679-x.

Li, B., Zhang, X. and Dong, Y. (2019) 'Nanoscale platforms for messenger RNA delivery', *Wiley Interdisciplinary Reviews: Nanomedicine and Nanobiotechnology*, 11(2), p. e1530. doi: 10.1002/WNAN.1530.

Liu, T., Liang, Y. and Huang, L. (2021) 'Development and Delivery Systems of mRNA Vaccines', *Frontiers in Bioengineering and Biotechnology*, 9, p. 718753. doi: 10.3389/FBIOE.2021.718753.

Maugeri, M. *et al.* (2019) 'Linkage between endosomal escape of LNP-mRNA and loading into EVs for transport to other cells', *Nature Communications*, 10(1), pp. 1–15. doi: 10.1038/s41467-019-12275-6.

Mecke, A. *et al.* (2005) 'Lipid bilayer disruption by polycationic polymers: the roles of size and chemical functional group', *Langmuir : the ACS journal of surfaces and colloids*, 21(23), pp. 10348–10354. doi: 10.1021/LA050629L.

Mendes, B. B. *et al.* (2022) 'Nanodelivery of nucleic acids', *Nature Reviews Methods Primers*, 2(1), pp. 1–21. doi: 10.1038/s43586-022-00104-y.

Meng, N. and Grimm, D. (2021) 'Membrane-destabilizing ionizable phospholipids: Novel components for organ-selective mRNA delivery and CRISPR–Cas gene editing', *Signal Transduction and Targeted Therapy*, 6(1), pp. 1–3. doi: 10.1038/s41392-021-00642-z.

Miah, K. M., Hyde, S. C. and Gill, D. R. (2019) 'Emerging gene therapies for cystic fibrosis', *Expert Review of Respiratory Medicine*, 13(8), pp. 709–725. doi: 10.1080/17476348.2019.1634547.

Mitchell, M. J. *et al.* (2020) 'Engineering precision nanoparticles for drug delivery', *Nature Reviews Drug Discovery*, 20(2), pp. 101–124. doi: 10.1038/s41573-020-0090-8.

Nakayama, Y. (2012) 'Hyperbranched polymeric "star vectors" for effective DNA or siRNA delivery', *Accounts of Chemical Research*, 45(7), pp. 994–1004. doi: 10.1021/AR200220T/ASSET/IMAGES/LARGE/AR-2011-00220T_0010.JPEG.

O'sullivan, M. J. and Lindsay, A. J. (2020) 'Molecular Sciences The Endosomal Recycling Pathway-At the Crossroads of the Cell', *International Journal of Molecular Sciences*, 21, pp. 1–21. doi: 10.3390/ijms21176074.

Pandey, A. P. and Sawant, K. K. (2016) 'Polyethylenimine: A versatile, multifunctional non-viral vector for nucleic acid delivery', *Materials Science and Engineering: C*, 68, pp. 904–918. doi: 10.1016/J.MSEC.2016.07.066.

Paramasivam, P. *et al.* (2021) 'Endosomal escape of delivered mRNA from endosomal recycling tubules visualized at the nanoscale', *Journal of Cell Biology*, 221(2), pp. 1–19. doi: 10.1083/jcb.202110137.

Patel, A. K. *et al.* (2019) 'Inhaled Nanoformulated mRNA Polyplexes for Protein Production in Lung Epithelium', *Advanced Materials*, 31(8), p. 1805116. doi: 10.1002/ADMA.201805116.

Patel, S. *et al.* (2017) 'Boosting Intracellular Delivery of Lipid Nanoparticle-Encapsulated mRNA', *Nano letters*, 17(9), pp. 5711–5718. doi: 10.1021/ACS.NANOLETT.7B02664.

Patel, S. *et al.* (2019) 'Brief update on endocytosis of nanomedicines', *Advanced Drug Delivery Reviews*, 144, pp. 90–111. doi: 10.1016/J.ADDR.2019.08.004.

Paunovska, K. *et al.* (2022) 'Drug delivery systems for RNA therapeutics', *Nature Reviews Genetics*, 23, pp. 265–280. doi: 10.1038/s41576-021-00439-4.

Ramachandran, S., Satapathy, S. R. and Dutta, T. (2022) 'Delivery Strategies for mRNA Vaccines', *Pharmaceutical Medicine*, 36(1), p. 11. doi: 10.1007/S40290-021-00417-5.

Rehman, Z. U., Hoekstra, D. and Zuhorn, I. S. (2013) 'Mechanism of polyplex- and lipoplex-mediated delivery of nucleic acids: Real-time visualization of transient membrane destabilization without endosomal lysis', *ACS Nano*, 7(5), pp. 3767–3777. doi: 10.1021/NN3049494/SUPPL_FILE/NN3049494_SI_010.AVI.

Rennick, J., Johnston, A. and Parton, R. (2022) 'Key principles and methods for studying the endocytosis of biological and nanoparticle therapeutics', *Nature Nanotechnology*, 16, pp. 266–276. doi: 10.1038/s41565-021-00858-8.

Du Rietz, H. *et al.* (2020) 'Imaging small molecule-induced endosomal escape of siRNA', *Nature Communications*, 11(1), pp. 1–17. doi: 10.1038/s41467-020-15300-1.

Sahay, G. *et al.* (2013) 'Efficiency of siRNA delivery by lipid nanoparticles is limited by endocytic recycling', *Nature biotechnology*, 31(7), pp. 653–658. doi: 10.1038/nbt.2614.

Sahay, G., Alakhova, D. Y. and Kabanov, A. V. (2010) 'Endocytosis of nanomedicines', *Journal of Controlled Release*, 145(3), pp. 182–195. doi: 10.1016/J.JCONREL.2010.01.036.

Sahin, U. *et al.* (2020) 'An RNA vaccine drives immunity in checkpoint-inhibitor-treated melanoma', *Nature*, 585(7823), pp. 107–112. doi: 10.1038/S41586-020-2537-9.

Schoenberg, D. R. and Maquat, L. E. (2012) 'Regulation of cytoplasmic mRNA decay', *Nature reviews. Genetics*, 13(4), pp. 246–259. doi: 10.1038/NRG3160.

Semple, S. C. *et al.* (2010) 'Rational design of cationic lipids for siRNA delivery', *Nature biotechnology*, 28(2), pp. 172–176. doi: 10.1038/nbt.1602.

Di Silvio, D. *et al.* (2019) 'Self-assembly of poly(allylamine)/siRNA nanoparticles, their intracellular fate and siRNA delivery', *Journal of Colloid and Interface science*, 557, pp. 757–766. doi: 10.1016/J.JCIS.2019.09.082.

Solomun, J. I. *et al.* (2021) 'Solely aqueous formulation of hydrophobic cationic polymers for efficient gene delivery', *International Journal of Pharmaceutics*, 593, p. 120080. doi: 10.1016/J.IJPHARM.2020.120080.

Suh, J. *et al.* (2012) 'Real-Time Gene Delivery Vector Tracking in the Endo-Lysosomal Pathway of Live Cells', *Microscopy Research and Technique2*, 75(5), pp. 691–697. doi: 10.1002/jemt.21113.

Sunshine, J. C., Peng, D. Y. and Green, J. J. (2012) 'Uptake and transfection with polymeric nanoparticles are dependent on polymer end-group structure, but largely independent of nanoparticle physical and chemical properties', *Molecular pharmaceutics*, 9(11), p. 3375. doi: 10.1021/MP3004176.

Tan, L. *et al.* (2020) 'Optimization of an mRNA vaccine assisted with cyclodextrin-polyethyleneimine conjugates', *Drug Delivery and Translational Research*, 10, pp. 678–689. doi: 10.1007/s13346-020-00725-4.

Taylor, D. (2015) 'The Pharmaceutical Industry and the Future of Drug Development', in *Pharmaceuticals in the Environment*. Royal Society of Chemistry, pp. 1–33. doi: 10.1039/9781782622345-00001.

Tros de Ilarduya, C., Sun, Y. and Düzgüneş, N. (2010) 'Gene delivery by lipoplexes and polyplexes', *European journal of pharmaceutical sciences*, 40(3), pp. 159–170. doi: 10.1016/J.EJPS.2010.03.019.

Vermeulen, L. *et al.* (2018) 'Endosomal Size and Membrane Leakiness Influence Proton Sponge-Based Rupture of Endosomal Vesicles', *ACS Nano*, 12, pp. 2332–2345. doi: 10.1021/acsnano.7b07583.

Vermeulen, L. M. P. *et al.* (2018) 'The proton sponge hypothesis: Fable or fact?', *European Journal of Pharmaceutics and Biopharmaceutics*, 129, pp. 184–190. doi: 10.1016/J.EJPB.2018.05.034.

Wadhwa, A. *et al.* (2020) 'Opportunities and Challenges in the Delivery of mRNA-based Vaccines', *Pharmaceutics*, 12(2). doi: 10.3390/PHARMACEUTICS12020102.

Wang, Wenxin *et al.* (2016) 'The transition from linear to highly branched poly(β-amino ester)s: Branching matters for gene delivery', *Science Advances*, 2(6). doi: 10.1126/SCIADV.1600102/SUPPL_FILE/1600102_SM.PDF.

Wu, Z. and Li, T. (2021) 'Nanoparticle-Mediated Cytoplasmic Delivery of Messenger RNA Vaccines: Challenges and Future Perspectives', *Pharmaceutical Research*, 38, pp. 473–478. doi: 10.1007/s11095-021-03015-x.

Xiao, B. *et al.* (2016) 'Combination Therapy for Ulcerative Colitis: Orally Targeted Nanoparticles Prevent Mucosal Damage and Relieve Inflammation', *Theranostics*, 6(12), pp. 2250–2266. doi: 10.7150/THNO.15710.

Xu, E., Saltzman, W. M. and Piotrowski-Daspit, A. S. (2021) 'Escaping the endosome: assessing cellular trafficking mechanisms of non-viral vehicles', *Journal of Controlled Release*, 335, pp. 465–480. doi: 10.1016/J.JCONREL.2021.05.038.

Yang, W. *et al.* (2023) 'Polymer-Based mRNA Delivery Strategies for Advanced Therapies', *Advanced Healthcare Materials*, p. 2202688. doi: 10.1002/ADHM.202202688.

Zhao, Tianyu *et al.* (2014) 'Significance of Branching for Transfection: Synthesis of Highly Branched Degradable Functional Poly(dimethylaminoethyl methacrylate) by Vinyl Oligomer Combination', *Angewandte Chemie*, 126(24), pp. 6209–6214. doi: 10.1002/ANGE.201402341.

Zheng, M. *et al.* (2021) 'Poly(α-l-lysine)-based nanomaterials for versatile biomedical applications: Current advances and perspectives', *Bioactive Materials*, 6(7), pp. 1878–1909. doi: 10.1016/J.BIOACTMAT.2020.12.001.

Zhu, J. *et al.* (2018) 'Dual-responsive polyplexes with enhanced disassembly and endosomal escape for efficient delivery of siRNA', *Biomaterials*, 162, pp. 47–59. doi: 10.1016/j.biomaterials.2018.01.042.

Zhu, Y. *et al.* (2022) 'RNA-based therapeutics: an overview and prospectus', *Cell Death & Disease*, 13(7), pp. 1–15. doi: 10.1038/s41419-022-05075-2.

Characterisation and Intracellular Mechanistic Analysis of Supramolecular, Cationic, mRNA-loaded Polyplexes for Efficient Transfection in HEK293T and A549 Cells.

Silvia Smith (stxss56@nottingham.ac.uk)

University of Nottingham, School of Biosciences, Sutton Bonington, LE12 5RD

MRes Biomolecular Technology: School of Pharmacy Research Project

Supervisor: Professor Cameron Alexander

Contents

Abstract

The demand for effective mRNA delivery methods has surged due to rapid developments in RNA therapeutics. Cationic polymers, forming protective mRNA complexes, have emerged as promising carriers. This study explores the transfection efficiency of supramolecular TETA-2L2 and TEPA-2L2 polyplexes within HEK293T and A549 cells, determined by luciferase assays and imaging GFP expression. The stability, size, surface charge and low cytotoxicity of these polyplexes were advantageous characteristics observed at the optimal nucleotide to polymer (N/P) ratios, around 8 to 16.

Understanding their uptake mechanisms and endosomal escape is crucial for tailoring therapeutic applications. This investigation indicates the involvement of multiple endocytic pathways for TETA-2L2 and TEPA-2L2 polyplex uptake. Observations of cells exposed to chloroquine revealed how the polyplexes rely on acidic environments for endosomal membrane destabilisation and efficient escape. Notably, variations in transfection efficiency were observed among different cell types, highlighting the significance of cell-specific considerations in polyplex design. Future research should focus on imaging uptake inhibition, evaluating co-localisation with endosomes and comparative assessments with other endosomal disruptive agents. These findings hold significant potential for advancing mRNA delivery methods required for therapeutic applications.

1. Introduction

The development of RNA therapeutics has developed rapidly since the FDA (U.S. Food and Drug Administration) approval and release of the Pfizer and Moderna COVID-19 messenger RNA (mRNA) vaccines. RNA therapeutics holds promise of pharmacological applications including cancer treatments (mRNA-encoded melanoma associated antigens (Sahin *et al.*, 2020)), protein replacement therapies (cystic fibrosis (Miah, Hyde and Gill, 2019)) and gene editing therapies (mRNA encoded DNA nucleases (Finn *et al.*, 2018) (Yang et al., 2023). However, the potential of RNA therapeutics hinges on the development of effective and safe mRNA delivery methods, primarily due to the inherent instability of naked mRNA *in vivo*.

One approach involves utilising cationic polymers that engage in electrostatic interactions with the negatively charged mRNA, condensing it into positively charged complexes (Paunovska *et al.*, 2022). These mRNA/polymer complexes protect the nucleic acids against enzymatic degradation by nucleases present in the bloodstream and extracellular fluids (Yudovin-Farber and Domb, 2006). Amongst other delivery systems, polymer-based carriers have gained prominence; their physical and chemical properties, such as, size, shape, surface charge, playing pivotal roles in facilitating transfection (Yudovin-Farber and Domb, 2006). Notable examples include polyethylenimine (PEI), poly(L-lysine), polyamides, chitosan and poly(β-amino ester) (PβAE) (Cordeiro *et al.*, 2017). Nonetheless, challenges of low transfection and concerns surrounding toxicity remain as barrier to clinical translation (Yue and Wu, 2013).

Through the interaction of these polymers with the plasma membrane, polyplexes are typically taken up by cells through endocytosis (Midoux *et al.*, 2008). To ensure successful transfection, polyplexes must escape the endosomal compartment, often relying on pH buffering capabilities, and release the mRNA into the cytosol before lysosomal degradation occurs (Patel *et al.*, 2017). Understanding these intricate intracellular mechanisms is essential for optimising polyplexes and helping reveal more about their structural-function relationships within biological systems, especially in diseased cells and tissues (Mendes *et al.*, 2022).

In previous laboratory work, two similar cationic polymers, denoted as TETA-2L2 and TEPA-2L2, demonstrated promising characteristics as vehicles for mRNA delivery. These linear, supramolecular polymers differ slightly in monomer chain length and the number of positively charged groups per repeating unit (+4 for TETA-2L2 and +5 for TEPA-2L2). Both monomers consist of low molecular weight polyamine chains terminated by two phenylalanine molecules, which serve as a cucurbituril (CB[8]) guest group. The interaction between phenylalanine and macrocyclic CB[8] enables polymerisation, as depicted in *figure 1.*

The present study investigates the influence of the ratio of negatively charged RNA to positively charged polymer (N/P ratio) on the transfection efficiency of TETA-2L2 and TEPA-2L2 polyplexes. These polyplexes exhibit characteristics such as long-term stability, a hydrodynamic diameter ranging from 30-60 nm, a zeta potential of +30 mV, and high *in vitro* transfection efficiency, contingent on the N/P ratio. Notably, polyplex transfection varies between cell types, as observed in HEK293T (human embryonic kidney 293) and A549 (lung cancer) cells, underscoring the importance of considering cell-specific mechanisms in polyplex design. Furthermore, the relatively low cytotoxicity of the polyplexes, when compared to the gold standard PEI (Bono *et al.*, 2020), further indicates their potential as effective carriers for therapeutic mRNA.

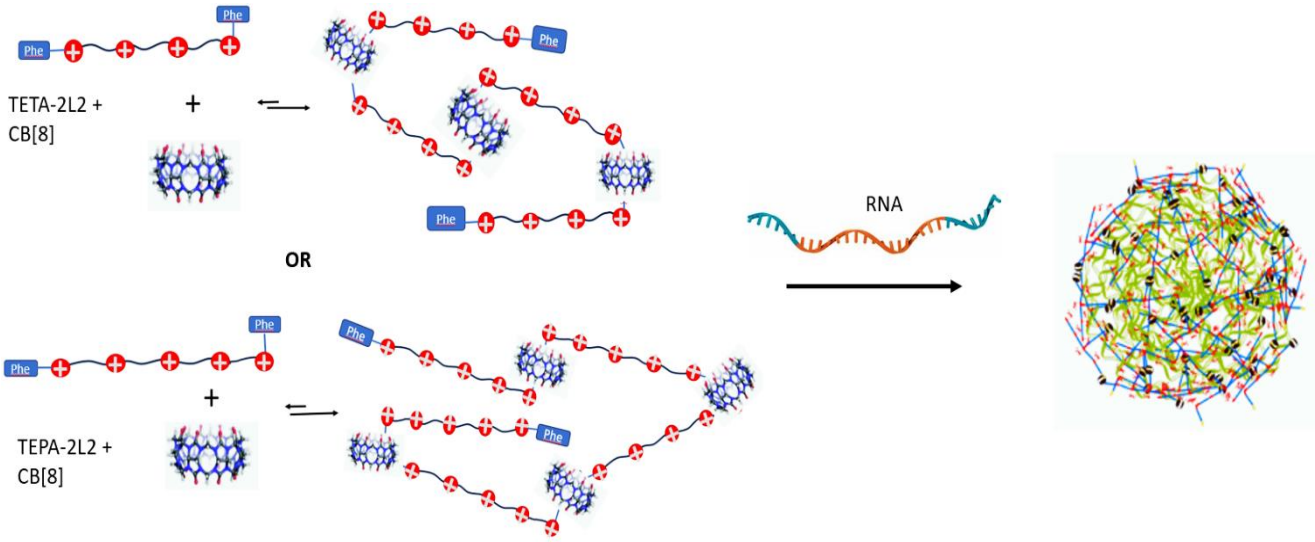

Figure. 1. *The polymerisation of TETA-2L2 and TEPA-2L2 using CB[8], facilitating the formulation of polyplexes with mRNA.*

Cell membranes, replete with anionic proteins and negatively charged phosphates in the glycerol backbone of the lipid bilayer (Zhang *et al.*, 2019), actively promote the uptake of cationic TETA-2L2 and TEPA-2L2 polyplexes. To gain deeper insights into the uptake mechanisms and intracellular pathways of these polyplexes, uptake inhibition analyses were conducted. Chlorpromazine and genistein, known inhibitors of the clathrin-mediated and caveolae-mediated endocytosis pathways, respectively, were used to decipher polyplex uptake routes in HEK293T cells. Eukaryotic cells employ distinct endocytic pathways for the internalisation of various substances, yielding different cellular outcomes (von Gersdorff *et al.*, 2006). Therefore, understanding how TETA-2L2 and TEPA-2L2 polyplexes are endocytosed across different cell lines is key for their optimisation for use in specfic therapeutic applications.

Additionally, to investigate the mechanisms enabling the escape of TETA-2L2 and TEPA-2L2 from endosomes, transfection experiments were conducted in the presence of chloroquine, a well-known endosome disruptive agent (Martinez *et al.*, 2020). The ability of chloroquine to buffer endosomal pH

(Solomon and Lee, 2009) and damage endosomal membranes (Du Rietz *et al.*, 2020) renders it an invaluable tool for studying endosome escape mechanisms. Chloroquine is known to prevent the fusion of endosomes and lysosomes, potentially inhibiting mRNA degradation within the acidic lysosomal environment (Varkouhi *et al.*, 2011). Hence, chloroquine has been employed to enhance the transfection efficiency of various gene delivery systems, including calcium phosphate, dextran and some liposomes (Cervia *et al.*, 2017). However, the impact of chloroquine on polymer-based methods remains a controversial subject in the literature, with studies reporting both positive (Erbacher *et al.*, 1995) and negative (Kichler *et al.*, 2001) effects on transfection.

Finally, cells transfected with fluorescently labelled polyplexes were monitored at various time points to track the stages of polyplex transfection. The findings from this study are poised to inform novel polymer design for nucleic acid delivery and contribute to the identification of the most efficient uptake and delivery mechanisms.

2. Materials and Methods

2.1. Cell culture

HEK293T (human embryonic kidney 293) cells were maintained in Dulbecco's modified Eagle's medium (DMEM; Sigma, D6429) enriched with 10% (v/v) Fetal Bovine serum (FBS; ThermoScientific, F7524) and 5 mg/mL L-glutamine (ThermoScientific, G7513). The mCherry-GAL9 HEK293T cell line was generated by Sal Jones (University of Nottingham) with plasmid #166689 (Addgene) following published procedure (Munson *et al.*, 2021).

A549 (lung cancer) cells (provided by Anna Grabowska's group) were cultured in DMEM, enriched with 10% (v/v) FBS and 5 mg/mL L-glutamine.

2.2. Polymer Synthesis

Low molecular weight polyamines, containing phenylalanine as CB[8] (Aqdot, AQ05010101)-guest group were synthesised by Rafal Kopiasz (University of Nottingham).

2.3. Formulation of polyplexes

A double concentrated solution of the polymer (concentration depends on N/P ratio) was prepared by adding Y µL of monomer+CB[8] stock to RNase-free water (Invitrogen, #AM9922).

$$Y(\mu\mathrm{L}) = \frac{\{\frac{(\frac{C_{RNA}}{Mw_{RNA} \times N/P})}{n_{charge} \times Mw_1}\}}{C_{stock} \times f}$$

where, C_{RNA} is the concentration of mRNA (either 5 or 30 µg/mL), Mw_{RNA} is the average molecular weight of RNA nucleotide (≈360 g/mol), N/P is the targeted N/P ratio, Mw_1 is the molecular weight of the repeating monomer unit within a polymer, n_{charge} is the number of positively charge groups per polymer's repeating unit and C_{stock} is the concentration of monomer+CB[8] stock solution (5 mg/mL).

All PEI polyplexes were prepared at N/P 8. TEPA-2L2 + CB[8] or TETA-2L2 + CB[8] were prepared at varying molar ratios to alter N/P to 1, 2, 4, 8, 12, 16, 24, 48 and 96.

A double concentrated solution of mRNA (twice the desired RNA concentration in polyplex) was prepared separately with RNase-free water. All polyplexes were prepared by mixing the solutions at a ratio of 1:1 volume quickly with pipette, approximately 15 times.

For characterisation studies, stock solutions polyplexes were prepared to have 30 µg/mL uncapped fLuc mRNA (provided by Centre for Process Innovation Limited) or 30 µg/mL GFP mRNA (TriLink, L-7201).

For *in vitro* transfection studies, stock solutions of the polymers were prepared to yield a final RNA concentration of 5µg/mL (100 ng mRNA/well). The double-concentrated mRNA solution was diluted 1:1 with RNase-free water to prepare naked mRNA samples of an equal concentration. Lipofectamine™ MessengerMAX™ (Invitrogen, #LMRNA) was prepared following manufacturer instructions, except diluted in reduced serum media, Opti-MEM (Gibco, #31985062).

*For Luciferase transfection assay***.** Nanoparticles were prepared using firefly luciferase (fLuc) mRNA (TriLink, L-7202).

For fluorescent imaging. Nanoparticles were prepared using a 1:4 ratio of Cy5-labelled, green fluorescent protein (GFP)-encoding mRNA (APExBIO, R-1011) and GFP-encoding mRNA (TriLink, L-7201). Polyplexes were assembled in the absence of light.

2.4. Characterisation of polyplexes

Polyplex size, polydispersity (PDI) and zeta potential were measured by dynamic light scattering (Zetasizer nanoseries, Malvern) at N/P ratios of 1, 2, 4, 8, 12 and 16 with the polyplex fixed at 30 µg/mL at 25 °C.

2.5. Treatment of cells with polyplexes

HEK293T cells were seeded at density of 25,000 cells per well, while A549 cells were seeded at 7,000 cells per well in complete DMEM, 24h prior to the polyplex treatment, using a clear 96-well plate (ThermoScientific, 167008). During treatment, the existing culture media was thoroughly aspirated and substituted with 200 µL of transfection media: 180 µL reduced serum media, Opti-MEM (Gibco, #31985062) and 20 µL of the polyplex solution (except for pre-prepared lipofectamine). This 1:9 dilution meant that 200 µL of 0.5 µg/mL mRNA was added to each pre-seeded well. The treated cells were then incubated at 37 °C and 5% CO_2 for different lengths of time depending on procedure.

2.5.1. *In vitro* Luciferase transfection assay

24h after treatment with nanoparticles, 200 µL transfection media was removed from each well, and replaced with 100 µL of diluted (1:1 with Opti-MEM) ONE-Glo™ D-luciferin substrate (Promega, #E6110). After incubation at 37 °C and 5% CO_2 (10 min), 90 µL of this was transferred to a white 96-well plate (Greiner, 655083) and analysed for relative luminescence (TECAN Spark 10M). Raw data was normalised to the Opti-MEM control average luminescence output.

2.5.2. *In vitro* Cytotoxicity Assay

24h after treatment with nanoparticles, 200 µL transfection media was removed from each well and replaced with pre-mixed 10 µL PrestoBlue™ reagent (ThermoFisher, #P50200) and 90 µL Phosphate-buffered saline (PBS). After incubation at 37 °C and 5% CO_2 (45 min), luminescence from each well was determined (TECAN Spark 10M) and normalised to the "killed" cells lysed with 1% Triton™. Metabolic activity was expressed as a percentage of the untreated, OptiMEM-only condition.

2.5.3. In vitro visualisation

The fluorophore, Hoechst 33342 (ThermoScientific, #62249) was used to stain cell nuclei. At specified time-points after treatment with polyplexes containing Cy5-labelled GFP-mRNA, samples were observed using a fluorescent microscope EVOS M5000 (EVOS Image Analysis software) or confocal microscope Leica SPE (LAS X software). Excitation/emission wavelengths used: Hoechst (370/450 nm); eGFP (488/507 nm); mCherry (587/610 nm) or TagRFP (555/584 nm); Cy5 (650/667 nm). Tiff files were exported to ImageJ for cropping and contrast adjustments.

2.5.4. Time-lapse Live Imaging

mCherry-Gal9 HEK293T cells were pre-seeded on a black 96-well plate (Greiner, #655891) at 25,000 cells per well and treated with polyplexes containing Cy5-labelled GFP-mRNA and Hoechst 33342.

Samples were observed using the ZEISS Celldiscoverer 7 automated microscope for live-cell imaging over 15 hours.

2.6. Blocking polyplex uptake using uptake inhibitors

Stock solutions of known inhibitors, chlorpromazine (ThermoScientific, #J63659) and genistein (ThermoScientific, #328270250), were prepared in PBS or dimethyl sulfoxide (DMSO), respectively, and stored per manufacturer's recommendation. Seeded HEK293T cells in complete DMEM were pre-treated with chlorpromazine or genistein at the indicated working concentration for 30 minutes. Later, the inhibitor solutions were removed and 150 µL of freshly prepared polyplexes treatments were added, containing the same inhibitor concentrations as used prior. Cells were incubated until a transfection assay was carried out, as described above. As a positive control, polyplexes without inhibitors were used to transfect cells.

2.7. Disruption of Endosomal acidification

Cells were treated with polyplex solutions containing endosome acidification inhibitor, chloroquine (ThermoScientific, J64459), at stated concentrations, and incubated at 37 °C and 5% CO_2.

2.8. Statistical Analysis

Data plots and statistics were performed using GraphPad Prism, version 10.0. Results are presented as means ± standard deviation values obtained from three technical repeats. Significant differences were identified using either multiple Student's *t*-tests, adjusted for multiple comparisons or two-way ANOVA with Tukey's post-hoc analysis. Differences were statistically significant at $p < 0.0.5$.

3. Results

3.1. Physicochemical characterisation of mRNA-loaded TETA-2L2 and TEPA-2L2.

With the aim of correlating physical properties with transfection capabilities, the sizes and surface charges of the formulations were characterised. The lower N/P ratios of TETA-2L2 and TEPA-2L2 result in a polyplex with negative surface charge (*figure 2A).* As N/P ratio increases, the excess of polymers on the surface of the polyplexes generated positively charged particles reaching a plateau of +30 mV at N/P 5.

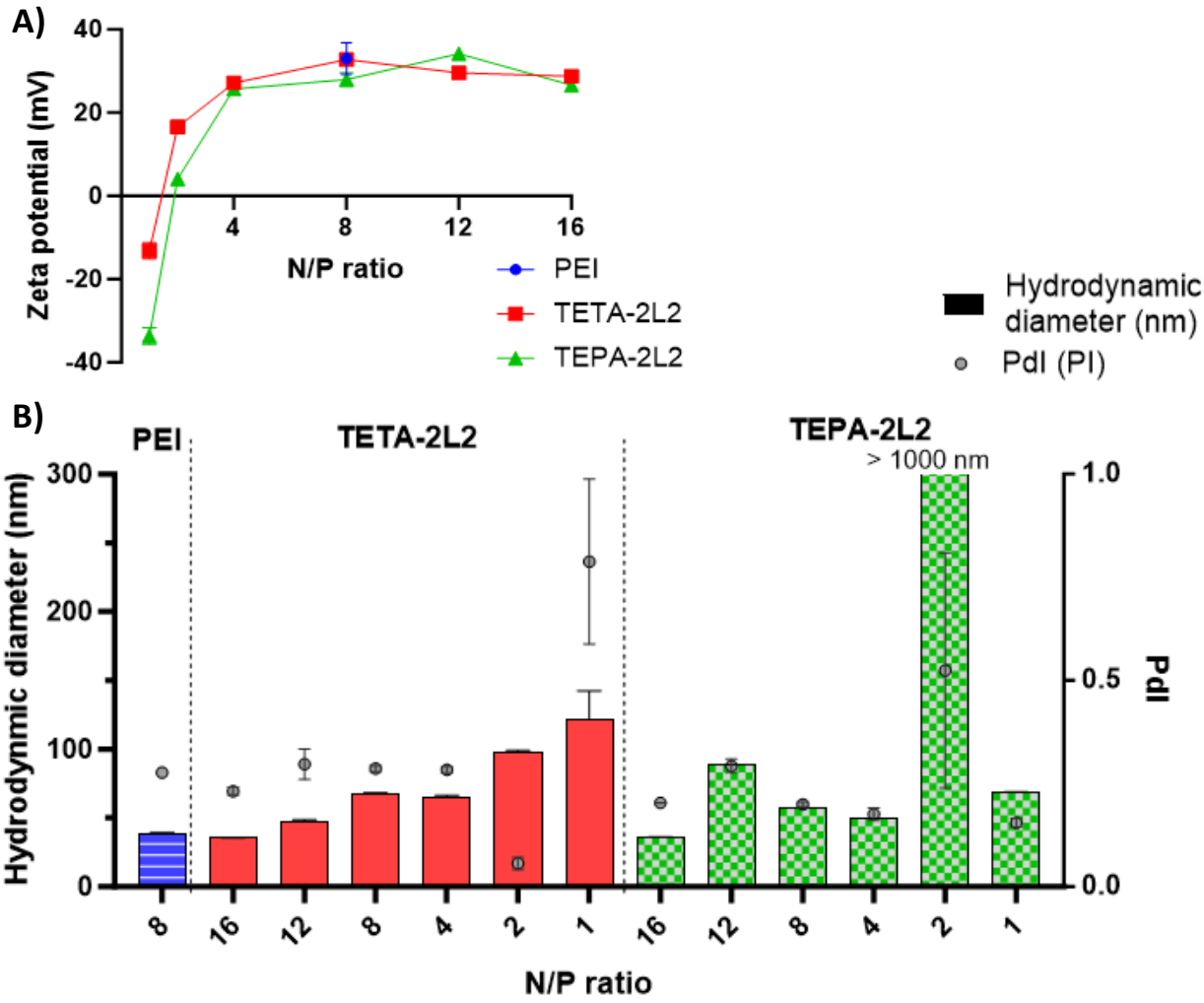

Figure. 2.A) *Zeta potential and* ***B)*** *average size measurements of TETA-2L2 and TEPA-2L2 nanoparticles complexed with fLuc mRNA. Mean ± SD, n = 3.*

The zeta potentials of TETA-2L2 N/P 1 and TEPA-2L2 N/P 2 were relatively close to 0 mV. This minimal electrostatic repulsion between polyplexes resulted in aggregation, thereby increasing the average particle size to >100 nm and polydispersity >0.6 (*figure 2B*). Above N/P ratio 2, the *fLuc*-mRNA/polyplexes were generally homogenous, with all average sizes below 100 nm (*figure 2B*). With increasing N/P ratio of TETA-2L2 polyplexes, polyplexes became more compact. However, this

relationship between N/P ratio and polyplex size was less linear for TEPA-2L2. The polydispersity index (PDI) for all polyplexes with a surface charge of +30 mV was below 0.3, signifying a narrow size distribution within the relatively homogenous population of polyplexes (*figure 2B*).

To confirm the impact of RNA type on polyplex size, the hydrodynamic diameters of TEPA-2L2 N/P ratio 8 and 16 were compared when complexed with either *GFP*-mRNA (996 base pairs) or *fLuc*-mRNA (1929 base pairs) (*figure 3*). A two-way ANOVA revealed that there was a statistically significant interaction between the effects of changing N/P ratio and complexed mRNA type ($F(1,8) = 1610$, $p < 0.0001$). Individually, both N/P ratio and complexed mRNA type showed to have a statistically significant effect on average size ($p < 0.0001$).

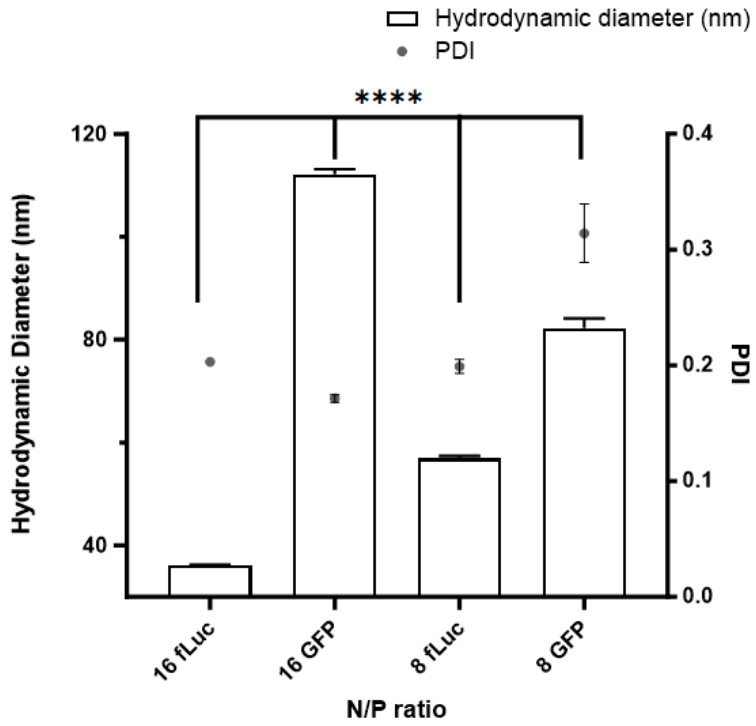

Figure. 3. *Average size and PDI comparison for TEPA-2L2 N/P 16 and 8 with either fLuc-mRNA or GFP-mRNA. Mean ± SD, n = 3, ****p < 0.0001.*

3.2. In vitro Transfection Efficiency of mRNA-loaded polyplexes in HEK293T depend on N/P ratio and mRNA type.

Following characterisation, the ability of the polyplexes to transfect cells was investigated. HEK293T cells were transfected by *fLuc*-mRNA/TETA-2L2 or *fLuc*-mRNA/TEPA-2L2 polyplexes at varying N/P ratios and their transfection activity was measured by quantitating luminescence generated by the expressed luciferase (*figure 2A*). There was no significant difference between polyplex structures for

each N/P ratio (mulitple unpaired t-tests: $p > 0.05$). The background signal from free, naked *fLuc*-mRNA-treated cells was used as the negative control. N/P ratios 1, 2, and 4 failed to transfect the HEK293T cells, and was not significantly different from the naked *fLuc*-mRNA (multiple unpaired t-tests: $p > 0.05$). Whereas N/P ratios 8, 12, 16, 24, 48 and 96 enabled *fLuc*-mRNA expression statistically significantly greater than the naked *fLuc*-mRNA (multiple unpaired t-tests: $p < 0.005$). All N/P ratios were significantly different from positive control PEI (mutliple unpaired t-tests: $p < 0.005$), except N/P 8 (unpaired t-test: $p = 0.37$). *Figure 4A* also reveals how the luciferase activity generated by *fLuc*-mRNA/polyplexes, for both TETA-2L2 and TEPA-2L2, at N/P ratios greater than 4 were the most comparable to positive controls (PEI and/or Lipofectamine) in HEK293T and the polyplexes below N/P 4, that also has a zeta potential less than +30 mV (*figure 2A*), failed to transfect cells.

A bell-shape profile was observed for the polyplex transfection efficiency at N/P ratios ranging from 1 to 96. For polyplexes greater than N/P 16, the luciferase activity remained approximately the same regardless of the further increase to N/P ratio (*figure 4A*). This indicates once the polyplex reached an N/P ratio of 24 or higher, any surplus polymers did not exert additional enhancement to transfection efficiency.

To investigate any cytotoxic effects of the polyplexes to HEK293T cells, the reducing power of living cells was determined by the PrestoBlue assay. A quantitative measure of viability (and cytotoxicity) is generated by harnessing this reducing power to convert resazurin to fluorescent resorufin. No cytotoxicity was found for the tested polyplexes; instead, metabolic activity was increased (*figure 4B).* As expected, the average metabolic activity of cells declined to approximately less than 80% of the level observed in the untreated cells following exposure to PEI polyplexes.

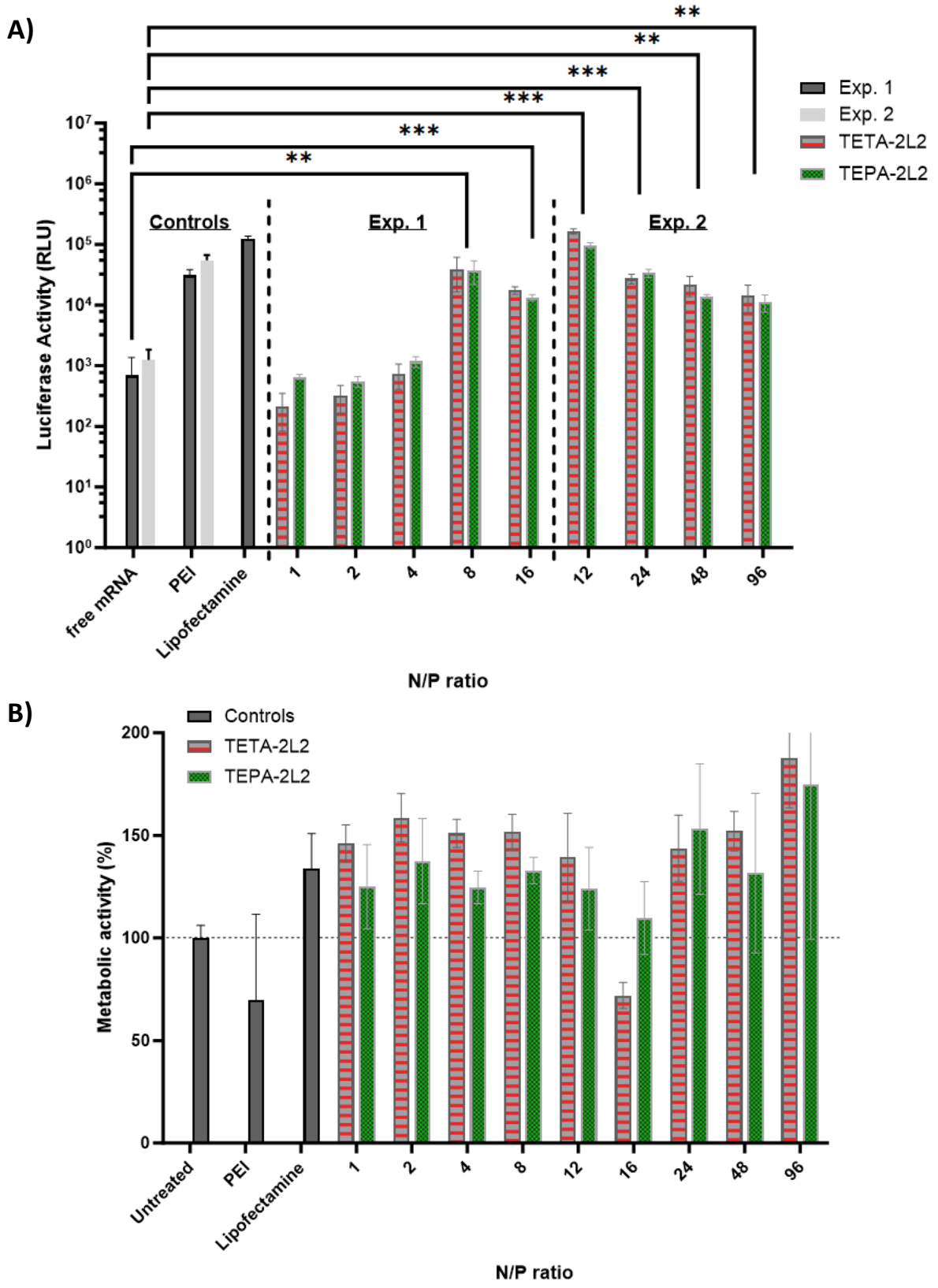

Figure. 4A) *N/P ratio dependent fLuc-mRNA expression in HEK293T 24 h post treatment with fLuc-mRNA/TETA-2L2 or fLuc-mRNA-TEPA-2L2. All data was normalised to untreated groups and free, naked mRNA was used as a negative control for background signal. Mean* ± SD, *n = 3 (technical repeats). **p < 0.005, ***p < 0.001.* ***B)*** *Cytotoxicity determined by PrestoBlue assay. Mean* ± SD. *Multiple unpaired t-test assessed statistical significance of chloroquine treatment (n = 3, *p < 0.05).*

To validate the mRNA delivery ability of the cationic polyplexes loaded with *GFP*-mRNA, the transfection efficiency was assessed in HEK293T cells using a fluoresence microscope, specifically examining the TETA-2L2 polyplex at an N/P ratio of 8. This polymer ratio was chosen due to its previously identified similarity in size, zeta potential and transfection efficiency to PEI. Naked *GFP*-mRNA-treated cells showed no GFP expression whilst the cells incubated with *GFP*-mRNA/TEPA-2L2 N/P 8 did show a GFP signal at 4 h post-treatment (*figure 5),* like PEI positive control. Transfection by both TEPA-2L2 and PEI polyplexes were slower than liposome Lipofectamine.

After 4 h, a smaller percentage of cells expressed GFP when transfected with TEPA-2L2 N/P 8 polyplexes compared to PEI. This was unexpected given the results of the luciferase assay (*figure 4A*) and may be an example of how mRNA type can impact transfection efficiency. Alternatively, transfection with TEPA-2L2 N/P 8 may just be slower than PEI within the first 4 h post-treatment.

Combined, these transfection results demonstrate how tuning the N/P ratio of TETA-2L2 and TEPA-2L2 enables the successful delivery of *fLuc*-mRNA or *GFP*-mRNA into HEK293T to be stably expressed into the Luciferase or GFP protein, respectfully, in the cytosol.

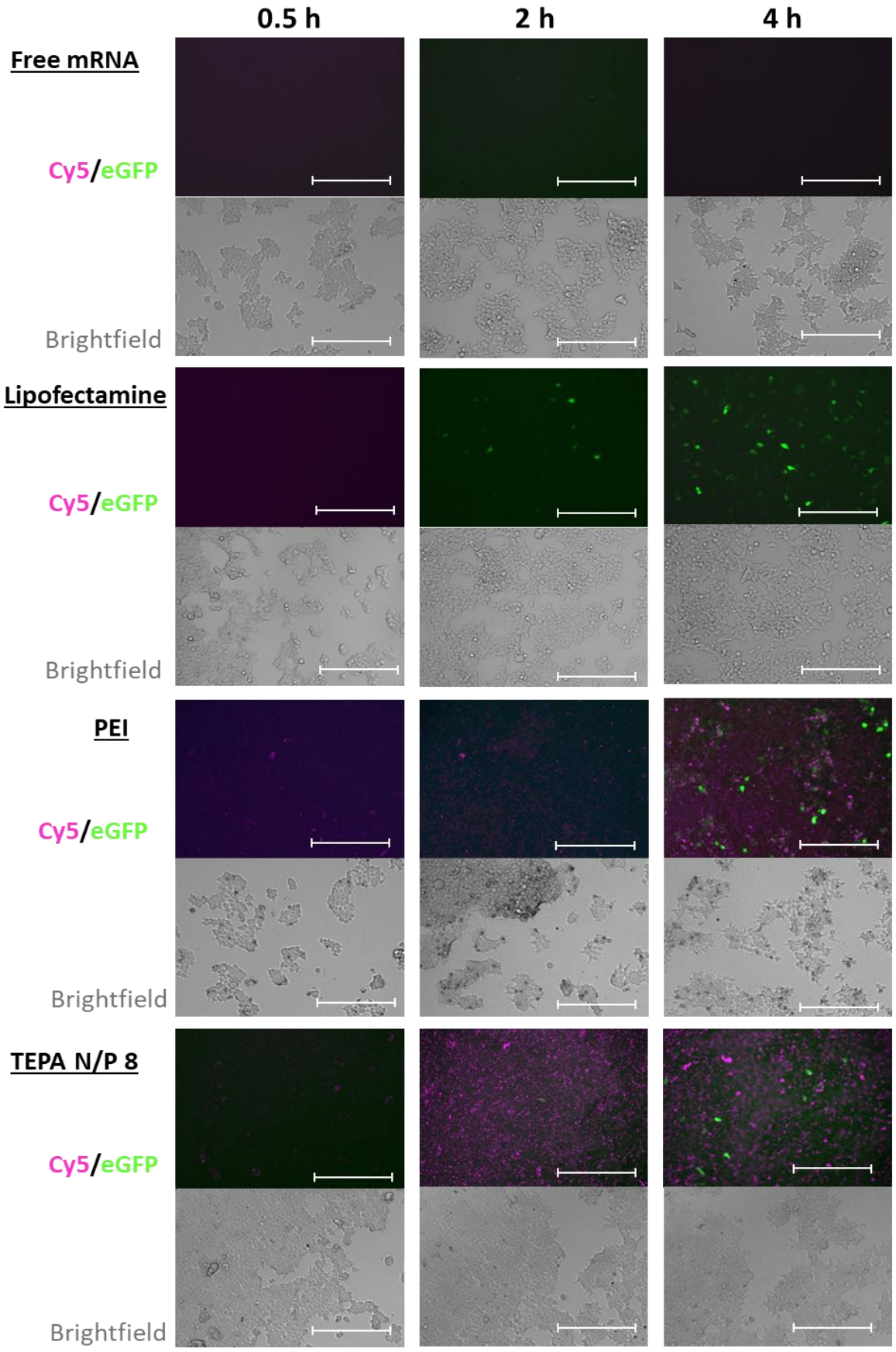

Figure. 5. *Fluorescent images of GFP-mRNA/TEPA-2L2 (magenta) uptake and early eGFP expression (green) within 4 hours after treatment of HEK293T cells. Positive control, Lipofectamine and negative control, naked mRNA. Scale bar = 300 µm.*

3.3. *In vitro* Transfection Efficiency of mRNA-loaded polyplexes depend on N/P ratio in A549.

The same luciferase experiment was conducted in the A549 cell line to observe any differences cell-type has on polyplex transfection. Like HEK293T, there was no significant difference in transfection efficiency between TETA-2L2 and TEPA-2L2 for both N/P 8 and N/P 16 (multiple unpaired t-tests: $p > 0.05$) in A549. These two N/P ratios were tested due to their success in HEK293T cells. Both N/P 16 and N/P 8 polyplexes generated luciferase activity significantly greater than naked mRNA (multiple unpaired t-tests: $p < 0.05$). N/P 16 was more potent than N/P 8 for the delivery of *fLuc*-mRNA, unlike in HEK293T.

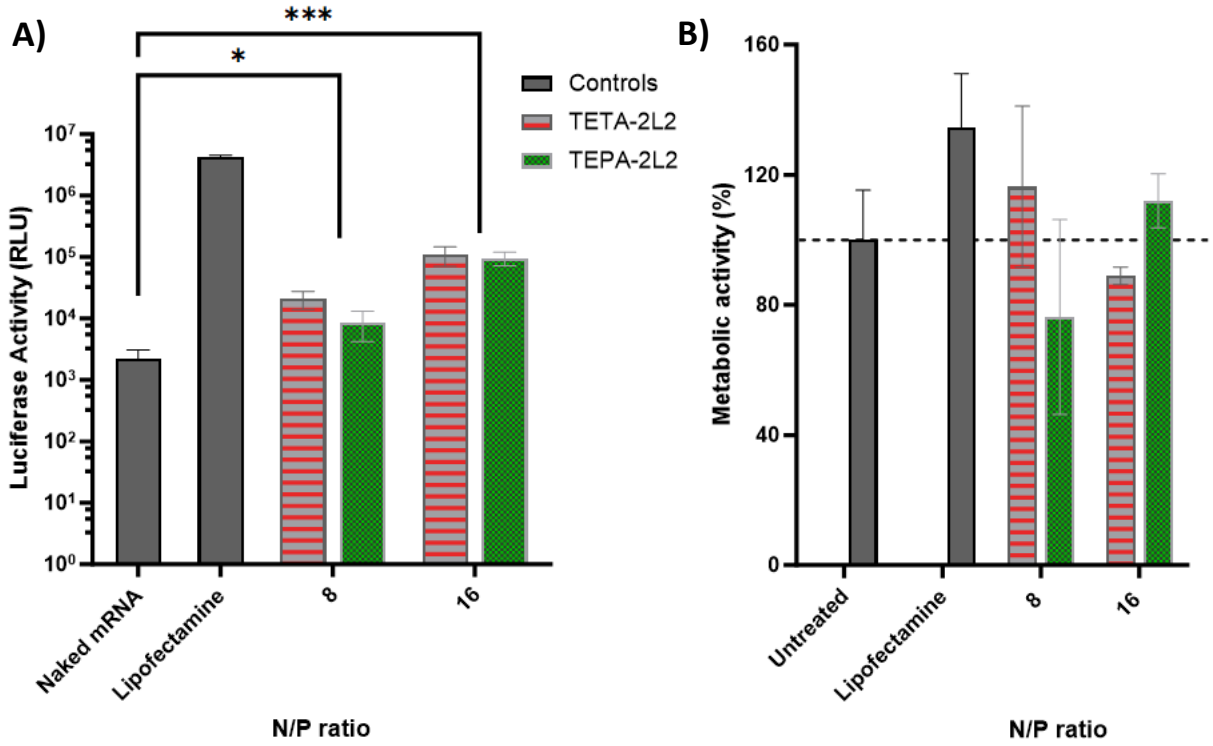

Figure. 6A. *N/P ratio dependent fLuc-mRNA expression in A549 24 h post treatment with fLuc-mRNA/Polyplexes. All data was normalised to untreated groups and free, naked mRNA was used as a negative control for background signal. Mean* ± SD, *n = 3 (technical repeats). *p < 0.05, ***p < 0.001.* ***B)*** *Cytotoxicity determined by PrestoBlue assay. Mean* ± SD. *Multiple unpaired t-test assessed statistical significance of chloroquine treatment (n = 3, *p < 0.05).*

As in HEK293T, the tested TETA-2L2 and TEPA-2L2 polyplexes showed minimal cytotoxicity (>80%) in A549 cells. There was no significant difference in metabolic activity caused by the polyplexes (*figure 6B).*

To directly visualise the difference between the potent transfection of N/P 16 against the poor transfection of N/P 8, GFP expression was observed in A549 cells after treatment with *GFP*-mRNA/TETA-2L2. According to *figure 7*, like the luciferase assay, the GFP expression enabled by TETA-

2L2 N/P 16 was greater than for TETA-2L2 N/P 8 in A549. Also, initial GFP expression was observed earlier (after 6 h) for TETA-2L2 N/P 16 than for TETA-2L2 N/P 8 (only after 22 h). The transfection efficiency of TETA-2L2 N/P 16 matched PEI in A549 cells (*figure 7*).

Figure 7 also demonstrates the intracellular distribution of polyplexes in A549 cells over time. At 2 h post-treatment with cationic polyplexes - PEI, TETA-2L2 N/P 8 and 16 - the polyplex signal (*magenta fluorescence*) was detected as punctuated fluorescence throughout the cytosol surrounding the cells. Whereas, after a 22 h incubation period, most of the Cy5-labelled mRNA appeared localised around the one side of the nuclei.

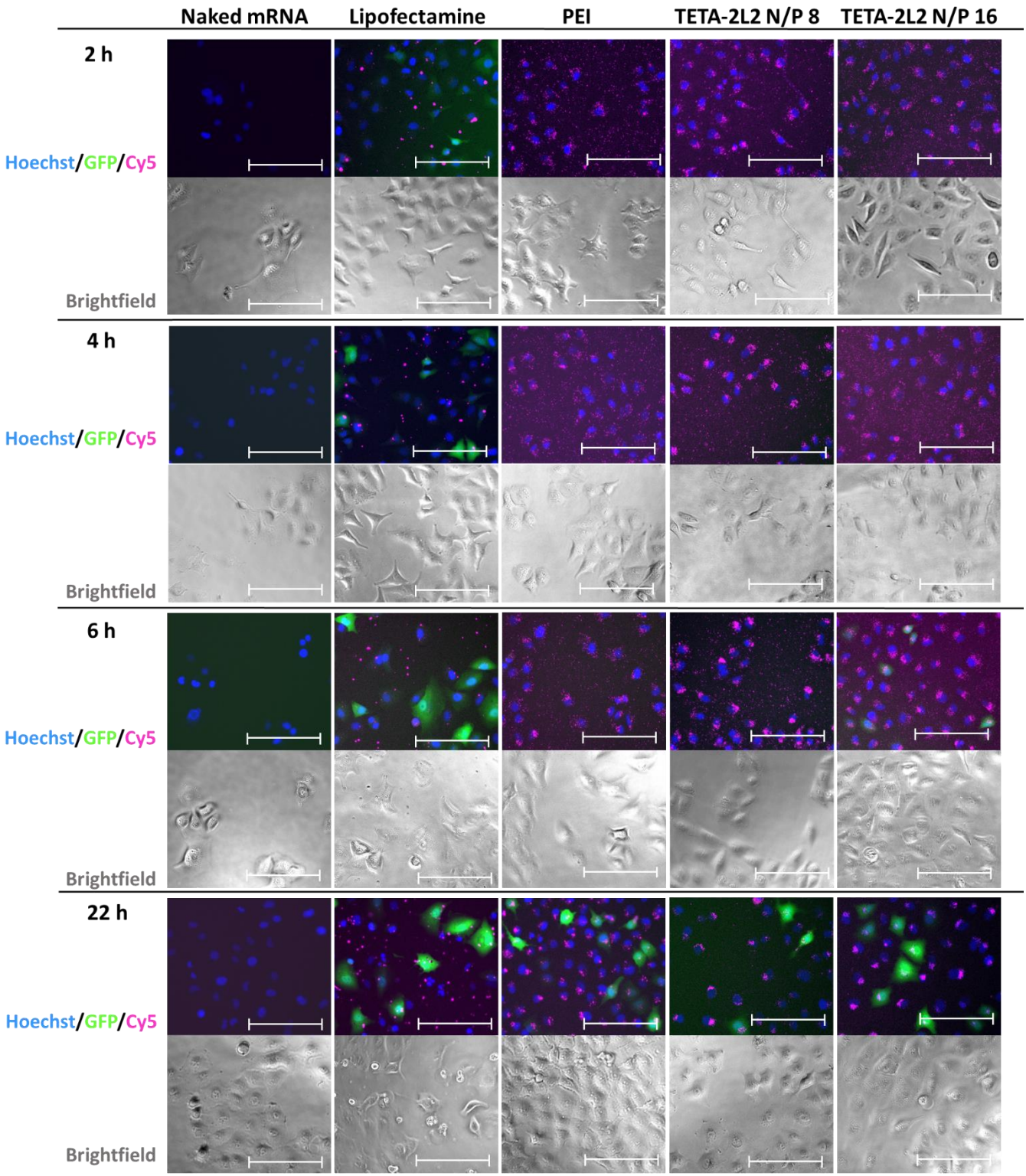

Figure. 7. *Fluorescent micrographs of A549 cells 2-, 4-, 6- and 22-hours post incubation with TETA-2L2 N/P 8, TETA-2L2 N/P 16 and positive controls, Lipofectamine or PEI, all complexed with Cy5-labelled GFP-mRNA (magenta). Cells were treated with naked Cy5-labelled GFP-mRNA as negative control. Cell nuclei labelled with Hoechst (blue). Scale bar = 150 µm.*

3.4. Polyplexes likely to be internalised by multiple mechanisms.

To gain insight into the relative contribution of different polyplex uptake pathways in HEK293T, cells were treated with either a clathrin-mediated endocytosis inhibitor (chlorpromazine) or caveolae-mediated endocytosis inhibitor (genistein). Neither inhibitor could significantly decrease the transfection efficiency of TETA-2L2 N/P 8 or TEPA-2L2 N/P 8 (*figure 8A*), unlike as for Lipofectamine. However, control TEPA-2L2 N/P 8 failed to transfect, potentially due to formulation error.

Also, the concentrations of inhibitors used showed greater than 20% cytotoxicity in HEK293T cells (*figure 8B and 8C*). Therefore, a more valid experiment would require a reduction in inhibitor concentration or washing cells with PBS after inhibitor treatment. Alternatively, flow cytometry would directly measure polyplex uptake whilst exposing cells to inhibitors for a shorter period.

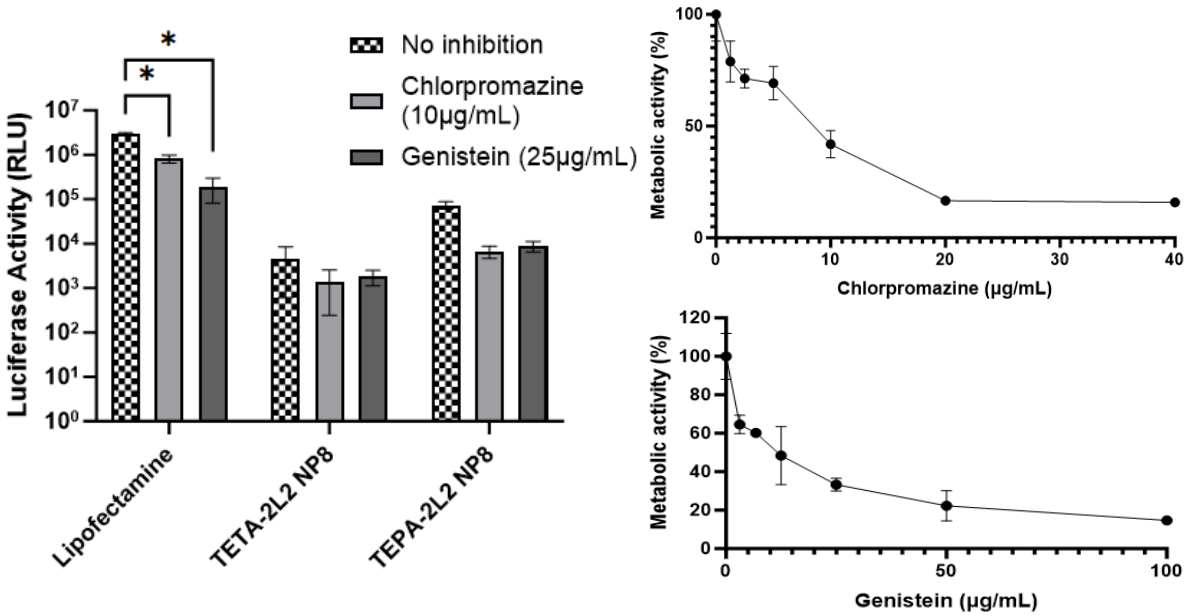

Figure. 8. A) *Effect of uptake inhibitors on the transfection of fluc-mRNA/TETA-2L2 and -TEPA-2L2 24 h post-treatment in HEk293T cells. Data shown as means ± SD, n = 3 (technical repeats). *p < 0.05. Cytotoxic effects to HEK293T cells after 24 h incubation with* ***B)*** *chlorpromazine and* ***C)*** *genistein.*

3.5. Polyplex intracellular trafficking visualised by fluorescent microscopy.

To explore the intracellular location of the polyplexes over time, A549 cells, transfected with TETA-2L2 N/P 16 and PEI polyplexes, were observed using a greater magnification (x40) than previously. This revealed a clear difference in the location of polyplexes (*magenta* representing Cy5-labelled mRNA *in figure 9*) at 2 h after treatment compared with 22 h after treatment. At 2 h, the polyplexes appeared more punctuated throughout the entire cell before becoming more organised around the

nuclei at 22h. This indicates localisation in certain cellular compartments. Additionally, as time progressed, the size of the visible *magenta spots* increased likely due to their coalescence.

In the cells expressing GFP, after transfection with PEI (*figure 9A*), the polyplexes appear more evenly distributed throughout the cell. This may be demonstrating the successful release of polyplexes into the cytosol from their contained compartments. However, this was not observed for the GFP-expressing cells after treatment with TETA-2L2 N/P 16 (*figure 9B*).

Another surprising observation was how TETA-2L2 N/P 16 polyplexes appear to interact with the nuclei after 22 h. There is a clear co-localisation between the Hoechst-stained DNA and Cy5-labelled polyplexes (*figure 9B*). Potentially, the polyplexes interact with the nuclei, condensing portions of the *blue*-stained DNA.

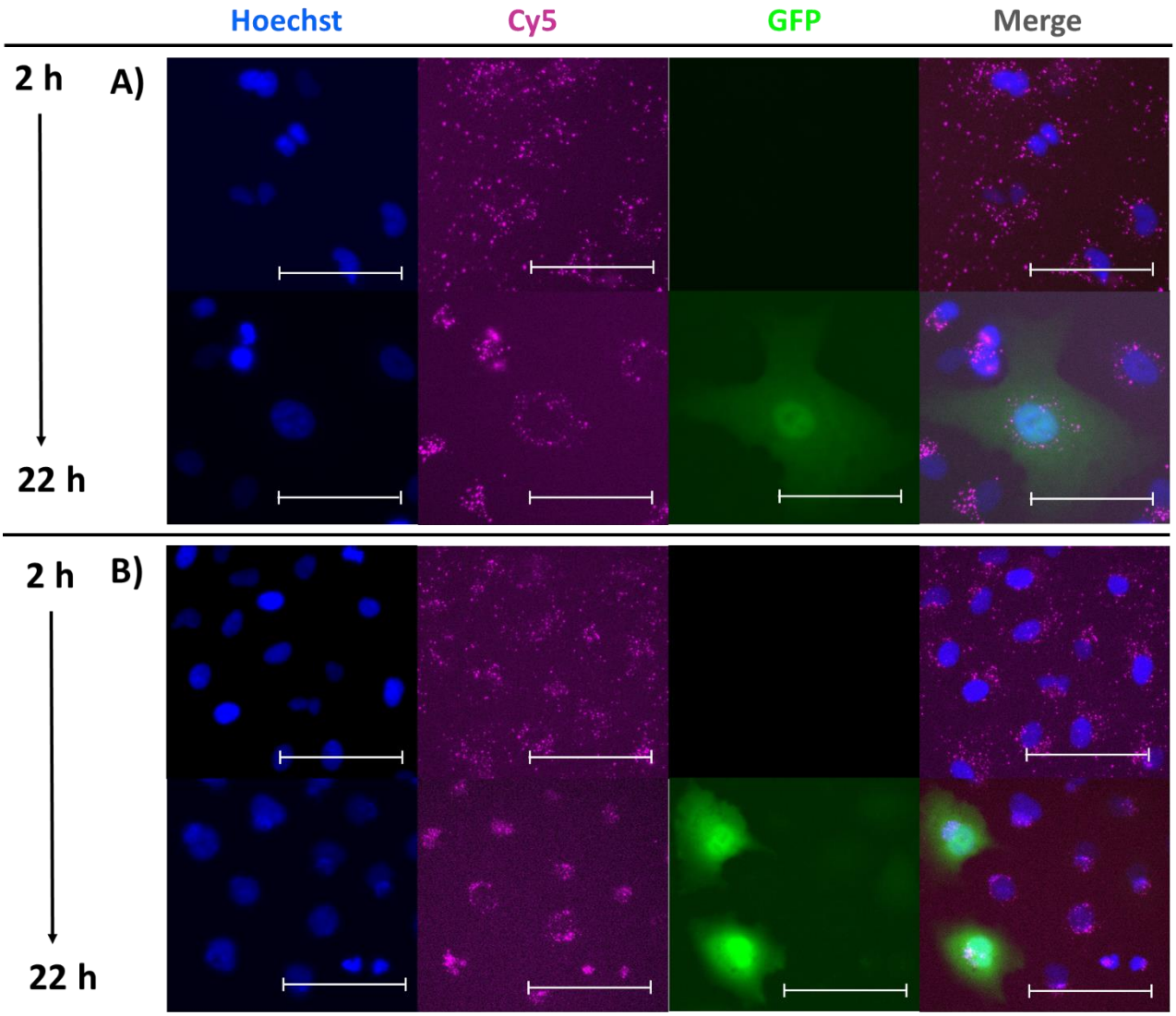

Figure. 9. *Confocal images of Cy5-labelled (magenta)* ***A)*** *GFP-mRNA/PEI and* ***B)*** *GFP/mRNA/TETA-2L2 N/P 16 in A549 cells. Hoechst-stained nuclei (blue). Scale bar = 75 µm.*

3.6. Chloroquine reduces Polyplex Transfection Efficiency in both HEK293T and A549.

To assess the involvement of endosomes and lysosomes in mRNA delivery, HEK293T and A549 cells were subject to transfection using TETA-2L2 or TEPA-2L2 polyplexes in the presence of chloroquine. Chloroquine, acting as a weak base, becomes protonated in the acidic environment of the endosomes and lysosomes, effectively buffering the pH within these compartments and preventing the fusion of endosomes and lysosomes (Solomon and Lee, 2009; Browning, 2014). Chloroquine has also been demonstrated to induce endosomal membrane damage, using fluorescently stained Gal9 as a sensor of this disruption. This is visualised as intracellular galectin foci by confocal microscopy (Du Rietz *et al.*, 2020). Theoretically, this should ensure polyplex formulations enter the cytosol where they can be translated.

Chloroquine did not improve the transfection efficiency of any N/P ratio of the TETA-2L2 or TEPA-2L2 polyplexes in HEK293T and A549 (*figure 7A; figure 9A).* This effect was similar for positive controls PEI and Lipofectamine. To confirm this decrease in transfection was not caused by the cytotoxic effects of chloroquine, a PrestoBlue metabolic activity assay *(figure 7B; figure 9B*) revealed the only significant toxic treatment combinations, with the addition of chloroquine, to be TETA-2L2 N/P 4 and TEPA-2L2 N/P 8 in HEK293T (multiple unpaired t-tests: $p < 0.05$). Therefore, the significant reduction in luciferase activity (*figure 7A*) of these polyplexes may have not been caused by the chloroquine alone.

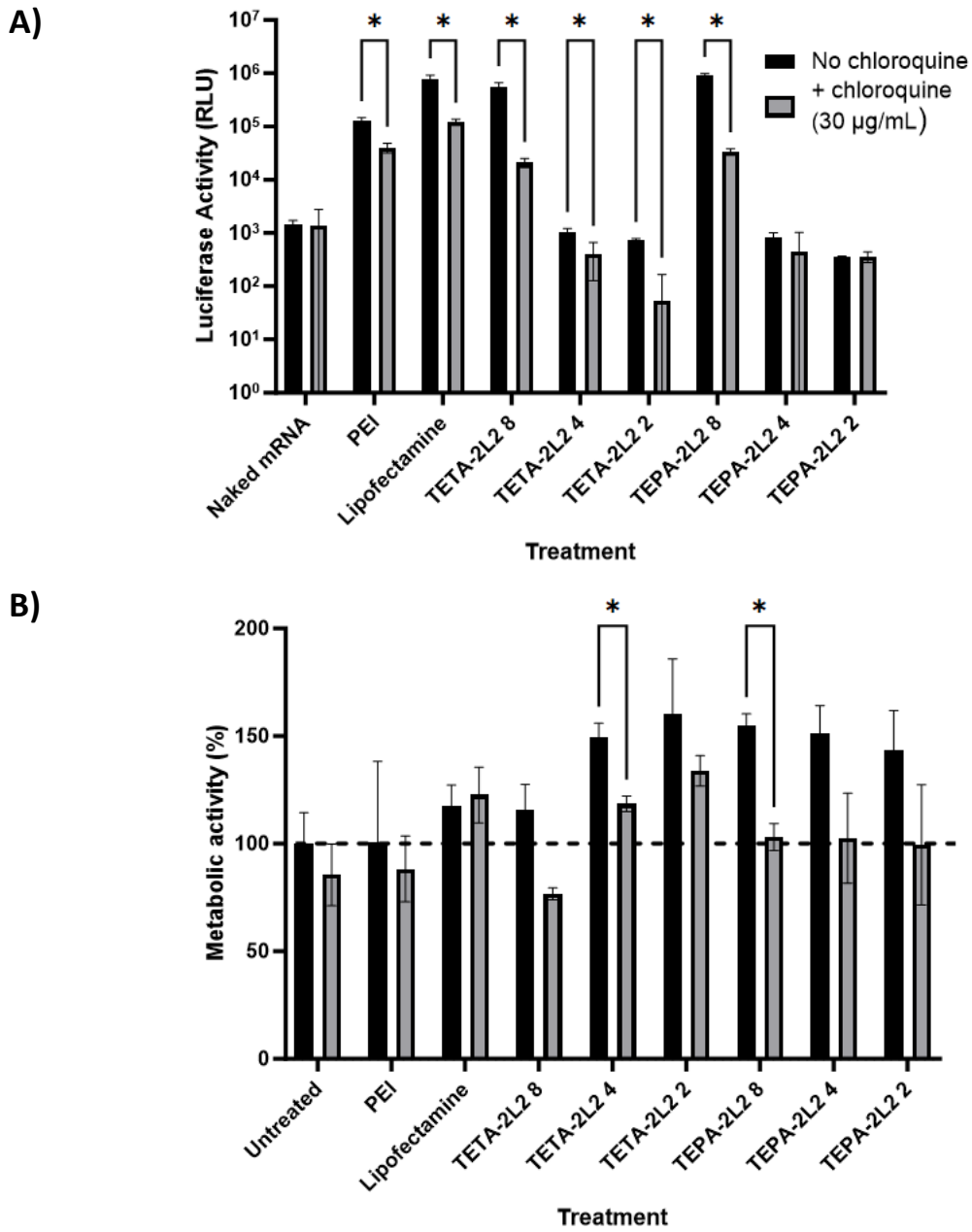

Figure. 10. *Effect of chloroquine (30 µg/mL) on* ***A)*** *the transfection efficiency and* ***B)*** *the metabolic activity measured by luciferase or PrestoBlue assay, respectively 24 h post-treatment with TETA-2L2, TEPA-2L2, PEI and Lipofectamine in HEK293T. Data presented as mean ± SD of 3 technical replicates, (n = 1). Asterisk (*) denotes a statistically significant difference compared to the original condition without chloroquine, determined using a two-tailed Student's t-test (*p<0.05).*

To investigate how chloroquine affects transfection within HEK293T cells further, mCherrry-Gal9 HEK293T cells were observed under a confocal microscope with various treatments. TEPA-2L2 N/P 8 was used due to its optimal luciferase activity (*figure 10A*). However, the GFP expression observed for TEPA-2L2 N/P 8 was less than expected (*figure 11*) and was dissimilar to that of the lipofectamine control. This could potentially be explained by the effect mRNA type has on polyplex size (*figure 3*).

Regardless, the same trend was observed, that, in the presence of chloroquine, the transfection efficiency of TEPA-2L2 N/P 8 was reduced to levels of no observable transfection.

The mCherry-Gal9 HEK293T cells were used to demonstrate the recruitment of Galectins to sites of endosomal damage. Gal9 was used over other galectins due to specificity in this function and its modification with an mCherry fluorescent label approximates endosomal escape events with the formation of an observable, bright red puncta under a microscope. Chloroquine induces this mCherry-Gal9 recruitment.

In the presence of chloroquine, many puncta were visible throughout the cells, and without chloroquine, the mCherry-Gal9s were evenly distributed throughout the entire cytosol of cells (*figure 11*). Surprisingly, there was no obvious relationship between increased endosomal damage and increased transfection for TEPA-2L2 N/P 8, therefore suggesting endosome escape is not a bottleneck for this polyplex.

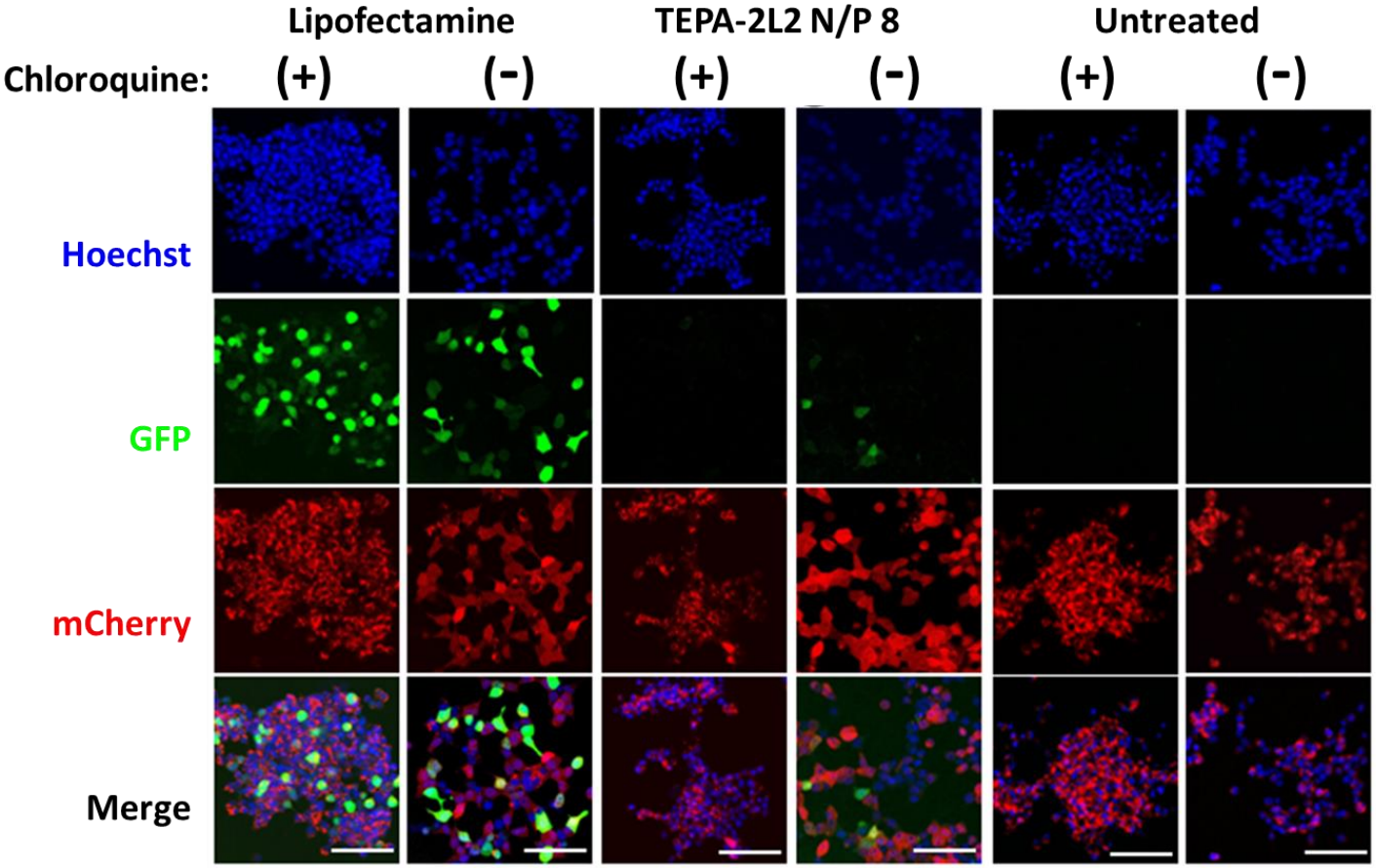

Figure. 11. *Confocal images of mCherry-Gal9 (red) HEK293T following 24 h incubation with GFP-mRNA complexed with TEPA-2L2 N/P 8, positive control (Lipofectamine) and untreated (OptiMEM) either with or without chloroquine (60 µg/mL), Hoechst-nuclei (blue), scale bar = 100 µm.*

A lack of red puncta was observed in the GFP-expressing cells after treatment with TEPA-2L2 N/P 8, in the absence of chloroquine. This would suggest that the polyplexes are either avoiding the endosomal

network all together, may be escaping later in the endosomal pathway, from lysosomes or cause unobservable endosome damage during their escape. However, the lack of observable puncta may also be a result of the low transfection efficiency.

A repeat of this experiment was completed using the CellDiscoverer 7 to track mCherry-Gal9 HEK293T cells at continuous time points (1-15 hours) throughout incubation, using TEPA-2L2 N/P 16 instead (*appendices 1*). Negative controls are not shown due to identicality with those in *figure 11*. As with TEPA-2L2 N/P 8, the transfection efficiency of TETA-2L2 N/P 16 was shown to decrease with chloroquine treatment.

In A549 cells, the chloroquine treatment was not significantly toxic (*figure 12B*) and therefore the reduction in transfection efficiency observed for TETA-2L2 N/P 16, N/P 8 and TEPA-2L2 N/P 16, were due to direct effects of chloroquine.

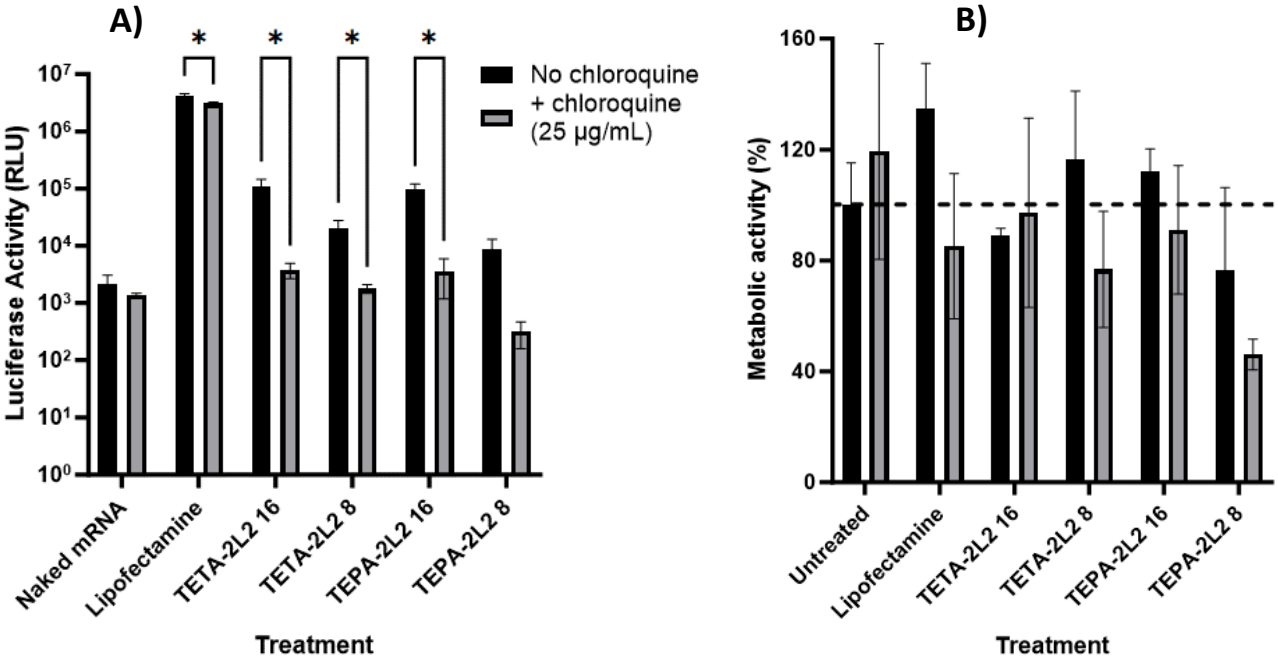

Figure. 12. *Effect of chloroquine (30 µg/mL) on* ***A)*** *the transfection efficiency and* ***B)*** *the metabolic activity measured by luciferase or PrestoBlue assay, respectively 24 h post-treatment with TETA-2L2, TEPA-2L2, PEI and Lipofectamine in A549. . Data presented as mean ± SD of 3 technical replicates, (n = 1). Asterisk (*) denotes a statistically significant difference compared to the original condition without chloroquine, determined using a two-tailed Student's t-test (*p<0.05).*

Again, these results were confirmed visually using a fluorescent microscope (*figure 13),* where GFP expression decreased for both TETA-2L2 N/P 16 and PEI in the presence of chloroquine. Negative controls were consistent with previous results. The images also revealed how chloroquine affects the intracellular location of the TETA-2L2 N/P 16 polyplexes. In the presence of chloroquine, the polyplexes appear more disperse throughout the cell in comparison to their perinuclear location when

chloroquine is absent. This is likely a visualisation of how chloroquine inhibits normal endosome/lysosome function and, thereby, normal intracellular trafficking of TETA-2L2 N/P 16..

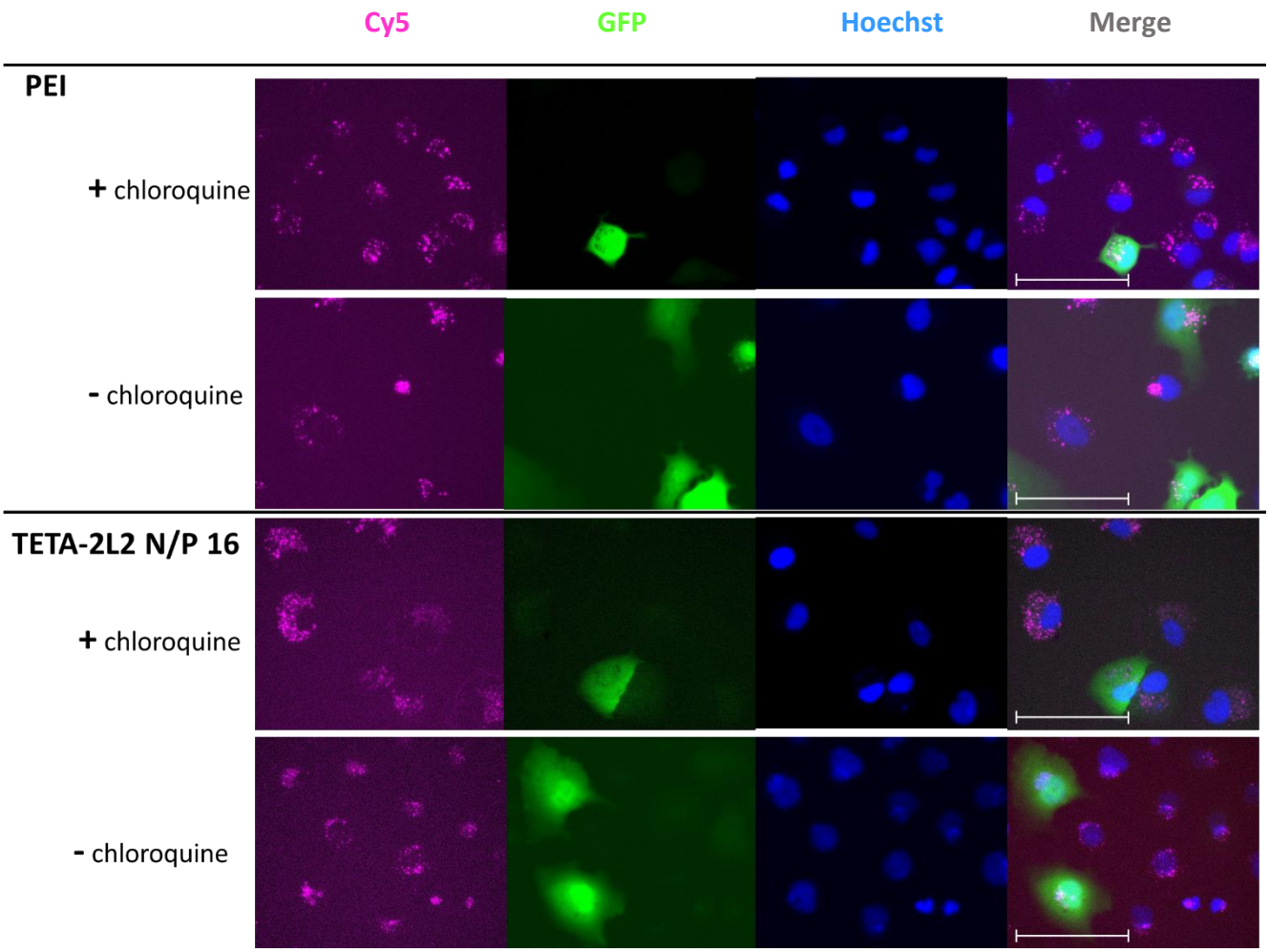

Figure. 13. *Fluorescent microscope images of HEK293T 22 h post-treatment with Cy5-labelled (magenta) GFP-mRNA complexed with TETA-2L2 N/P 16 and positive control (PEI) either with or without chloroquine (30 µg/mL), cell nuclei stained with Hoechst (blue), scale bar = 75 µm.*

4. Discussion

This objective of this study was to gain a deep insight into the promising behaviour of TETA-2L2 and TEPA-2L2 as mRNA delivery systems by comparing cellular events, encompassing aspects like uptake and endosomal escape. Additionally, their overall transfection efficiency and cytotoxicity in comparison to established delivery systems, PEI and Lipofectamine were assessed.

At N/P ratios higher than 2, TETA-2L2 and TEPA-2L2 could condense mRNA into nanoparticles with hydrodynamic diameters around 30-90 nm and zeta potential approximately +30 mV; both of which proved beneficial to efficient endocytosis and mRNA delivery. This size range (<100 nm) allows for

proper endocytosis (Delafosse, Xu and Durocher, 2016) and a relatively high zeta potential of approximately ± 30 mV is critical for ensuring robust physiochemical stability within a colloidal suspension. This substantial repulsive force acting between polyplexes effectively prevents aggregation, which might otherwise occur due to intermittent collisions with adjacent polyplexes (Zielínska *et al.*, 2020). Additionally, the synthesis of TETA-2L2 and TEPA-2L2 polymers and their formulation with mRNA successfully generated polyplex solutions with low polydispersity (0.1-0.3). This relatively monodisperse size distribution is key for therapeutic delivery (Hickey *et al.*, 2015).

The transfection assays revealed no substantial differentiation between TETA-2L2 and TEPA-2L2 in either cell line (*figure 4A; 6A*), despite previous research suggesting that shorter polycations could enhance mRNA expression by minimising electrostatic interactions between the carrier and mRNA (Bettinger *et al.*, 2001). The absence of this effect may be attributed to the already short nature of both TETA-2L2 and TEPA-2L2 monomers.

The transfection efficiency for different N/P ratios were tested to optimise this critical parameter for TETA-2L2 and TEPA-2L2 polyplexes. The results indicated the important role N/P ratio plays in improving the transfection ability of the polyplexes, and how the optimal N/P ratio varies with different cell lines (HEK293T and A549). The transfection efficiency of mRNA/TETA-2L2 and mRNA/TEPA-2L2 were both generally found to increase with N/P ratio. Increasing the ratio of polycations with respect to a fixed amount of mRNA was likely to have improved transfection due to the higher density of positive charge assisting with uptake and/or promoting release of polyplexes from endo-lysosomal vesicles (Thibault *et al.*, 2011). Similarly, a high N/P ratio for PEI (approximately N/P 8) was previously identified for efficient transfection whilst lower N/P ratios reduced nucleic acid delivery (Démoulins *et al.*, 2016).

Nevertheless, an increase in polymer content beyond an N/P ratio of 16 within TETA-2L2 and TEPA-2L2 polyplexes resulted in a decrease in luciferase expression (as depicted in *figure 4A*) in HEK293T. This outcome was likely attributed to the excess polymer failing to facilitate efficient mRNA release whilst also causing increased cytotoxicity (Almulathanon *et al.*, 2018).

When comparing against the positive controls, there were some differences in the transfection efficiency across the luciferase assay compared to imaging GFP expression whilst using the same N/P ratio. Polyplex characterisation revealed that *fLuc*-mRNA, with its higher nucleotide count and charge density, possessed a smaller size compared to the relatively larger *GFP*-mRNA/polyplex. In a previous comparative analysis of polymers complexed with distinct RNA species, namely mRNA (2,000 nucleotides) and replicon RNA (7,000 nucleotides), it became evident that the optimal polymer composition varied depending on the length and structural characteristics of the RNA (Blakney *et al.*,

2018). This observation helps elucidate the variations in N/P ratios observed when TETA-2L2 and TEPA-2L2 were complexed with either *fLuc*-mRNA or *GFP*-mRNA. Consequently, it is imperative to tailor the delivery system appropriately to accommodate these slight structural disparities (Blakney *et al.*, 2018).

Another observation identified that there were no obvious patterns of successful transfection amongst cells when transfected with either *GFP*-mRNA⁄TETA-2L2 or *GFP*-mRNA⁄TEPA-2L2. It is unclear whether transfection is based on unknown chance events or potentially dependent on the cell cycle phase, as has been mentioned previously (Männisto *et al.*, 2005). Despite the existing research being limited to DNA/polyplexes, studies suggest that, as well as nuclear entry, differences in transfection are also caused by cell-cycle-dependent processes including endocytosis, intracellular distribution, and protein expression. This is important to consider for *in vivo* experiments with mRNA/polyplexes where a large fraction of target cells within organisms are nondividing (Brunner *et al.*, 2000).

Mechanistic investigations propose that the transfection efficiency and cytotoxicity of cationic polymers are connected and likely stem from the interactions of polymers with biological membranes (Grandinetti, Smith and Reineke, 2011). For example, the ability of PEI to promote nucleic acid expression is linked to its cytotoxicity (Vaidyanathan, Orr and Banaszak Holl, 2016) as also demonstrated in *figure 4A* and *4B.* However, for TETA-2L2 and TEPA-2L2, there was no relationship between an increased transfection efficiency of certain N/P ratios and the detrimental effect caused to the transfected cells. Instead of cell death, the metabolic activity of HEK293T and A549 cells both typically increased upon transfection (figure 4B; 6B). The differing results observed can be ascribed to the intrinsic characteristics of the polymers, given that polyplexes of PEI and TETA-2L2 or TEPA-2L2 exhibited similar size and zeta potential values at an N/P ratio of 8 (*figure 2*). This measurement of metabolic activity reflects the increase in reducing power of cells, which is affected by several factors including changes to cellular oxidoreductase activity, mitochondrial activity, intracellular trafficking, polyplex metabolic behavioural deviations and many more (Luzak, Siarkiewicz and Boncler, 2022). Or, the presence of the polyplexes and increased ion availability may reduce the cell stress caused by the untreated, OptiMEM-only condition (Rashid and Coombs, 2019). Either way, the increased metabolic activity may not accurately represent the cell viability after treatment with the polyplexes.

Polyplex cytotoxicity can be modulated by the established method of altering amphiphilicity through either a covalent or non-covalent attachment of polyethylene glycol (PEG). This improves the balance between cationic charge and hydrophobicity which is key for the safe and effective delivery of nucleic acids (Samal *et al.*, 2012). One study, testing PEG-modified PEI, revealed an enhanced transfection efficiency without increasing cell toxicity of PEI, *in vitro* (Tang *et al.*, 2003) whilst another identified a

toxicity reduction of PEI at the correct PEGylation degree and N/P ratio (Fitzsimmons and Uludağ, 2012). Following this study, PEGylation of TETA-2L2 and TEPA-2L2 should be explored.

Understanding the mechanisms of cellular uptake of TETA-2L2 and TEPA-2L2 is a key aspect in developing their transfection efficiency further. It is important to determine the level of particle uptake in relation to mRNA expression (Ulkoski *et al.*, 2021). Various micrographs demonstrate how the Cy5-labelled mRNA/polyplexes increased in cellular fluoresence overtime, implying a continuous polyplex uptake (*figure 5; 7*). *Figure 7* also reveals how initial uptake occurs after two hours, but complete uptake (i.e., no Cy5-mRNA/polyplexes visible in the solution surrounding the cells) does not occur until 6 hours after treatment with TETA-2L2 N/P 8 and TETA-2L2 N/P 16. Flow cytometry would confirm which N/P ratio enables the highest rate of particle uptake after a specified amount of time (Bishop *et al.*, 2016) as it is difficult to accurately determine whether particles are indeed present inside or outside of cellular membrane with fluorescent imaging alone (Ulkoski *et al.*, 2021).

There are many factors that are involved in deciding the uptake pathway of nanoparticle delivery systems, including particle size, surface charge, stability, cell type and culture conditions (Xiang *et al.*, 2012). The neutral net charge of the low N/P ratios of TETA-2L2 and TEPA-2L2 (*figure 2A*) inhibited uptake due to polyplex aggregation and lack of membrane association; hence, the importance of maintaining polyplex surface charge throughout treatment. Anionic molecules present in the *in vitro* transfection medium, or remnants from the growth medium may alter polyplex surface charges and increase aggregation (Pezzoli *et al.*, 2017). This would reduce polyplex uptake and limit their transfection potential (Merkel *et al.*, 2011). Once more, modifying polyplexes with PEG can offer a solution to this issues, owing to its strong hydrophilic properties, electrical neutrality, and steric-repulsive tendencies (Shi *et al.*, 2021).

In a previous study, the uptake efficiency of nanoparticles measuring 20 and 40 nm in diameter exceeded that of 100 nm nanoparticles in endothelial cells by a factor of 5-10 times (Wang *et al.*, 2009). This was generally the case for TETA-2L2 and TEPA-2L2 polyplexes, where the smaller, more monodisperse N/P ratios had the greater transfection efficiency. The small size of the polyplexes successfully transfecting cells (30-60 nm for N/P ratio 8-16) may suggest which endocytic pathway is utilised by cells for uptake; nanoparticles approximately 60 nm in size will use caveolin-mediated pathway, whereas nanoparticles approximately 100 nm in size utilise the clathrin-mediated pathway (Rennick, Johnston and Parton, 2022).

Polyplexes likely utilise multiple uptake mechanisms for cellular internalisation, and their intracellular fates are usually relevant to the uptake pathways (Khalil *et al.*, 2006). This appeared to be the case for TETA-2L2 and TEPA-2L2, as neither chlorpromazine or genistein significantly reduced their

transfection efficiency (*figure 8A*), suggesting that both clathrin-mediated and caveolae-mediated endocytosis are involved in polyplex uptake. Similar results have been discovered for PEI, with hypotheses stating that polyplex uptake was mediated by endocytosis pathways (von Gersdorff *et al.*, 2006; Benfer and Kissel, 2012). Or, potentially, these uptake data imply the involvement of another uptake mechanism, such as micropinocytosis (Hufnagel *et al.*, 2009) but this is rarely reported for polyplexes. Alternatively, the inhibitor concentration may have been too low to fully inhibit uptake across all cells. Future work should focus on imaging this uptake inhibition as done previously using other nanoparticles (Garaiova *et al.*, 2012).

A dependence on the cell type was also identified for PEI uptake (Rejman, Bragonzi and Conese, 2005). The slight differences in the cell membranes of different mammalian cells should be considered when examining polyplex uptake. For example, previous studies provide indirect evidence of caveolae involvement in PEI uptake (Kichler *et al.*, 2001). HepG2 cells lack endogenous caveolins (Fujimoto *et al.*, 2000) and when transfected with PEI, showed low transfection efficiency compared to HEK293T cells, suggesting PEI internalisation by caveolae-mediated endocytosis is required to achieve efficient gene transfer. The varying outcomes of N/P ratio for TETA-2L2 and TEPA-2L2 polyplexes across HEK293T and A549 cells may therefore be attributed to disparities in their unique uptake mechanisms. Consequently, these findings provide opportunities for tailoring polyplexes to suit specfic cell types and applications (Silva *et al.*, 2022).

Following cellular uptake, polyplexes encapsulated within a vesicular structure, most likely the endosome, which subsequently merges with the lysosome. The progressive expansion of the fluorescent Cy5-mRNA/polyplex “spots” observed over time in *figure 7 and 9B* suggests a potential increase in the presence of vesicles or vesicle fusion. During the journey from initial uptake to lysosomal entrapment, polyplexes experience a shift in pH, transitioning from the physiological pH to a more acidic environment, typically around pH 5. An examination of the various micrographs revealed that, at least 6 hours after treatment, the majority of polyplexes are concentrated within closely adjacent cellular compartments, likely indicative of lysosomal localisation. Or, the conspicuous presence of large Cy5-labelled structures could signify polyplex aggregation within the intracellular environment (Ulkoski *et al.*, 2021).

Within the A549 cells incubated with TETA-2L2 N/P 16 for 22 h, the Cy5-labelled polyplexes were detected mainly around the nuclei, indicating transport of polyplexes towards the perinuclear region *(figure 9B*). This was not observed in HEK293T cells and therefore indicates the differences that exist in intracellular processing of polyplexes between different cell types (Wilschut *et al.*, 2009). Therein,

these differences may contribute to transfection efficiency and help explain the variation observed in A549 and HEK293T regarding the optimal N/P ratio of polyplex.

The co-localisation between polyplexes and nuclear contents at 22 hours after treatment with TETA-2L2 N/P 16 was apparent in isolated cells as well as transfected cells (*figure 9B*). It has been previously hypothesised that since cationic polymers can disrupt the endosomal membrane, they may also be capable of disrupting the nuclear envelope (Grandinetti, Smith and Reineke, 2011). However, in the absence of any further evidence, these findings appear artefactual. Therefore, further study on polyplex interactions with the nuclear membrane in A549s is necessary. This ability to permeabilise the nuclear membrane would be desirable for therapeutics involving DNA delivery but must consider the cytotoxic effects as a result.

The polyplexes must escape endosomal compartments before lysosomal degradation (Jones *et al.*, 2013). The mechanism of endosome escape for polyplexes is greatly speculated with the most supported mechanism to-date being the bursting of endosomes caused by the 'proton sponge effect'. This described phenomenon is triggered by the protonation of polymer amine groups which slows endosomal acidification, causing an influx of ions followed by increase in osmotic pressure (Wu and Li, 2021). However, various studies have disproved that PEI utilise this mechanism for endosome escape (Benjaminsen *et al.*, 2013). The findings in f*igure 9B* demonstrate how there was no discernible distribution of Cy5-labelled polyplexes throughout the GFP-expressing cells following treatment with TETA-2L2 N/P 16. This observation aligns with the hypothesis that the polyplexes do not induce the bursting of endosomes but rather imply a more gradual release of polyplexes into the cytosol.

An alternative hypothesis for endosome escape has been formulated to suggest that either the protonatable imidazole groups or secondary amines of PEI can destabilise membranes, thereby creating pores facilitating the translocation of nucleic acids into the cytosol (Démoulins *et al.*, 2016). Regardless of the mechanism, it is clear the buffering capacity of PEI is responsible for inducing endosomal escape (He *et al.*, 2013). As polyplexes are transported to the lower pH environments, their overall increase in positive charge likely contributes to this membrane destabilisation (Griffiths *et al.*, 2007).

Nonetheless, it is important to acknowledge that the escape of all nanoparticles from endosomes is inherently an inefficient process (Sahay *et al.*, 2013; Maugeri *et al.*, 2019). This is demonstrated by the proportion of GFP-expressing relative to the number of cells displaying Cy5-mRNA/polyplex uptake in *figures 5, 7, 9 and 13.* Therefore, any modification aimed at mitigating factors that impede endosome escape should yield significant enhancements to the transfection efficiency of cationic polymers.

In the presence of chloroquine, a reduction in the transfection efficiencies of both TETA-2L2 and TEPA-2L2 was observed when compared to their counterparts in the absence of chloroquine. This effect as consistent across HEK293T and A549 cells (*figures 10A; 12A*). However, this outcome was not considered for TETA-2L2 N/P 4 and TEPA-2L2 N/P 8 in HEK293T cells due to the significant cytotoxicity associated with the chloroquine and polyplex treatment combination (*figure 10B*).

This general finding for TETA-2L2 and TEPA-2L2 suggest that the polyplexes may indeed benefit from progressing into the acidic pH of the late endosome and lysosome. It is plausible that the surplus polymer linked with the N/P ratios greater than 4 may necessitate a lower pH environment than that provided by the early endosome to facilitate membrane permeability and mRNA decomplexation (Almulathanon *et al.*, 2018). The normal functioning of acidic organelles appears pivotal in creating an environment conductive to the effective delivery of mRNA into the cytosol by TETA-2L2 and TEPA.

Furthermore, these results raise the possibility that an early release of polyplexes from the endosome may be 'outweighed' by the necessity for a more acidic pH environment for the release of polyplexes from late endocytic vesicles (Funhoff *et al.*, 2004). This notion was supported by the examination of mCherry-Gal9 HEK293T cells in *figure 11 and appendix 1*, which did not reveal a clear correlation between chloroquine-triggered endosome damage (*shown as red puncta*) and an increase in GFP expression following transfection with TEPA-2L2 N/P 8 or TEPA-2L2 N/P 16.

Similar results have been found for other cationic polymers (Gu *et al.*, 2016) including PEI (Rittner *et al.*, 2002). A possible explanation for this observation may be related to the inherent ability of PEI to independently induce endosomal escape prior to reaching the lysosomal stage (Cervia *et al.*, 2017), albeit the precise mechanisms remain unidentified.

This decrease in transfection efficiency in the presence of chloroquine was also found for another bio-reducible polymer (Kim *et al.*, 2011). The study hypothesised that these bio-reducible polymers also have their own ability for endosome escape by acting as an endosome buffer. However, it was also theorised that chloroquine could displace polycations from the complexed nucleic acids in polyplexes (Cheng *et al.*, 2006). This would lead to an increased exposure of dissociated nucleic acids to nuclease enzymes, resulting in less mRNA expression. Both theories could be plausible for the decreased transfection of TETA-2L2 and TEPA-2L2 in the presence of chloroquine.

In theory, the slowing down of endosome acidification by chloroquine can be beneficial for polyplexes that need to escape in a small window of the endosome pathway. However, this effect may not be as beneficial for those polyplexes requiring a lower pH to escape during later stages in endosomal maturation (Thibault *et al.*, 2016). As depicted in *figure 13*, the presence of chloroquine appears to

lead to a more widespread distribution of Cy5-mRNA polyplexes throughout each of the A549 cells compared to the conditions without chloroquine. This illustrates the effects of chloroquine in A549 cells and could signify either endosome bursting or a failure of endosomes to fuse with lysosomes.

The effect of chloroquine on the transfection efficiency of TETA-2L2 and TEPA-2L2 suggest untimely endosome escape compromises mRNA delivery efficiency (Hu *et al.*, 2019). Therefore, TETA-2L2 and TEPA-2L2 polyplexes need to be more finely tuned to better escape independently. More research is required to elucidate the molecular mechanism of TETA-2L2 and TEPA-2L2 endosome/lysosome escape to realise their full potential as polymer-based nucleic acid delivery systems.

Conclusions

Overall, the findings of this study indicate the promise of TETA-2L2 and TEPA-2L2 as effective carriers for mRNA delivery into cells. Their characterisation revealed that polyplexes within the size range of 30-60 nm and possessing a zeta potential of approximately +30 mV exhibited successful transfection of cells. Although the optimal N/P ratio varied depending on the cell type, it was consistently most efficient within the N/P 8 to 16 range, with these polyplexes appearing to be just as efficient as standard PEI polyplexes.

The uptake studies suggested the involvement of multiple endocytic pathways, while investigation into endosome disruption with chloroquine suggested that polyplexes likely utilise acidic environments to escape into the cytosol through the destabilisation of endo/lysosomal membranes. Importantly, these transfection processes occurred without causing acute toxicity to cells, *in vitro*, as PEI did.

All data were collected from technical repeats ($n = 3$) within a single experiment. To further validate these initial findings and gain a more comprehensive understanding, future research should involve biological replicates. Additional investigations, such as exploring flow cytometry, detailed co-localisation with endo/lysosomes, and assessing the endosome buffering capacity of these polyplexes, will further elucidate the intracellular mechanisms at play. These insights hold great potential for advancing the field of mRNA delivery and its therapeutic applications.

References

Almulathanon, A. A. Y. *et al.* (2018) 'Comparison of Gene Transfection and Cytotoxicity Mechanisms of Linear Poly(amidoamine) and Branched Poly(ethyleneimine) Polyplexes', *Pharmaceutical Research*, 35(4), pp. 1–12.

Benfer, M. and Kissel, T. (2012) 'Cellular uptake mechanism and knockdown activity of siRNA-loaded biodegradable DEAPA-PVA-g-PLGA nanoparticles', *European Journal of Pharmaceutics and Biopharmaceutics*, 80(2), pp. 247–256.

Benjaminsen, R. V. *et al.* (2013) 'The Possible "Proton Sponge " Effect of Polyethylenimine (PEI) Does Not Include Change in Lysosomal pH', *Molecular Therapy*, 21(1), pp. 149–157.

Bettinger, T. *et al.* (2001) 'Peptide-mediated RNA delivery: a novel approach for enhanced transfection of primary and post-mitotic cells', *Nucleic Acids Research*, 29(18), p. 3882.

Bishop, C. J. *et al.* (2016) 'Quantification of cellular and nuclear uptake rates of polymeric gene delivery nanoparticles and DNA plasmids via flow cytometry', *Acta biomaterialia*, 37, pp. 120–130.

Blakney, A. K. *et al.* (2018) 'One Size Does Not Fit All: The Effect of Chain Length and Charge Density of Poly(ethylene imine) Based Copolymers on Delivery of pDNA, mRNA, and RepRNA Polyplexes', *Biomacromolecules*, 19(7), pp. 2870–2879.

Bono, N. *et al.* (2020) 'Non-Viral in Vitro Gene Delivery: It is Now Time to Set the Bar!', *Pharmaceutics*, 12(183), pp. 1-23.

Browning, D. J. (2014) 'Pharmacology of Chloroquine and Hydroxychloroquine', *Hydroxychloroquine and Chloroquine Retinopathy*, p. 35-63.

Brunner, S. *et al.* (2000) 'Cell cycle dependence of gene transfer by lipoplex, polyplex and recombinant adenovirus', *Gene therapy*, 7(5), pp. 401–407..

Cervia, L. D. *et al.* (2017) 'Distinct effects of endosomal escape and inhibition of endosomal trafficking on gene delivery via electrotransfection', *PLoS ONE*, 12(2).

Cheng, J. *et al.* (2006) 'Structure-function correlation of chloroquine and analogues as transgene expression enhancers in nonviral gene delivery', *Journal of medicinal chemistry*, 49(22), pp. 6522–6531.

Cordeiro, R. A. *et al.* (2017) 'High transfection efficiency promoted by tailor-made cationic tri-block copolymer-based nanoparticles', *Acta Biomaterialia*, 47, pp. 113–123.

Delafosse, L., Xu, P. and Durocher, Y. (2016) 'Comparative study of polyethylenimines for transient gene expression in mammalian HEK293 and CHO cells', *Journal of biotechnology*, 227, pp. 103–111.

Démoulins, T. *et al.* (2016) 'Polyethylenimine-based polyplex delivery of self-replicating RNA vaccines', *Nanomedicine: Nanotechnology, Biology and Medicine*, 12(3), pp. 711–722.

Erbacher, P. *et al.* (1995) 'Glycosylated polylysine/DNA complexes: gene transfer efficiency in relation with the size and the sugar substitution level of glycosylated polylysines and with the plasmid size', *Bioconjugate chemistry*, 6(4), pp. 401–410.

Finn, J. D. *et al.* (2018) 'A Single Administration of CRISPR/Cas9 Lipid Nanoparticles Achieves Robust and Persistent In Vivo Genome Editing', *Cell reports*, 22(9), pp. 2227–2235.

Fitzsimmons, R. E. B. and Uludağ, H. (2012) 'Specific effects of PEGylation on gene delivery efficacy of polyethylenimine: Interplay between PEG substitution and N/P ratio', *Acta Biomaterialia*, 8(11), pp. 3941–3955.

Fujimoto, T. *et al.* (2000) 'Isoforms of caveolin-1 and caveolar structure', *Journal of cell science*, 113 Pt 19(19), pp. 3509–3517.

Funhoff, A. M. *et al.* (2004) 'Endosomal Escape of Polymeric Gene Delivery Complexes Is Not Always Enhanced by Polymers Buffering at Low pH', *Biomacromolecules,* 5(1), pp. 32-9.

Garaiova, Z. *et al.* (2012) 'Cellular uptake of DNA–chitosan nanoparticles: The role of clathrin- and caveolae-mediated pathways', *International Journal of Biological Macromolecules*, 51(5), pp. 1043–1051.

von Gersdorff, K. *et al.* (2006) 'The internalization route resulting in successful gene expression depends on both cell line and polyethylenimine polyplex type', *Molecular therapy : the journal of the American Society of Gene Therapy*, 14(5), pp. 745–753.

Grandinetti, G., Smith, A. E. and Reineke, T. M. (2011) 'Membrane and Nuclear Permeabilization by Polymeric pDNA Vehicles: Efficient Method for Gene Delivery or Mechanism of Cytotoxicity?', *Molecular Pharmaceutics*, 9, pp. 523-538.

Griffiths, P. C. *et al.* (2007) 'Studies on the mechanism of interaction of a bioresponsive endosomolytic polyamidoamine with interfaces. 1. Micelles as model surfaces.', *Biomacromolecules*, 8(3), pp. 1004–1012.

Gu, J. *et al.* (2016) 'Factors influencing the transfection efficiency and cellular uptake mechanisms of Pluronic P123-modified polypropyleneimine/pDNA polyplexes in multidrug resistant breast cancer cells', *Colloids and Surfaces B: Biointerfaces*, 140, pp. 83–93.

He, Y. *et al.* (2013) 'Polyethyleneimine/DNA polyplexes with reduction-sensitive hyaluronic acid derivatives shielding for targeted gene delivery', *Biomaterials*, 34(4), pp. 1235–1245.

Hickey, J. W. *et al.* (2015) 'Control of polymeric nanoparticle size to improve therapeutic delivery', *Journal of controlled release : official journal of the Controlled Release Society*, 219, pp. 536–547.

Hu, Y. *et al.* (2019) 'Peptide-grafted dextran vectors for efficient and high-loading gene delivery', *Biomaterials Science*, 7(4), pp. 1543–1553.

Hufnagel, H. *et al.* (2009) 'Fluid phase endocytosis contributes to transfection of DNA by PEI-25', *Molecular therapy : the journal of the American Society of Gene Therapy*, 17(8), pp. 1411–1417.

Jones, C. H. *et al.* (2013) 'Overcoming nonviral gene delivery barriers: perspective and future', *Molecular pharmaceutics*, 10(11), pp. 4082–4098.

Khalil, I. A. *et al.* (2006) 'Uptake pathways and subsequent intracellular trafficking in nonviral gene delivery', *Pharmacological reviews*, 58(1), pp. 32–45.

Kichler, A. *et al.* (2001) 'Polyethylenimine-mediated gene delivery: a mechanistic study', *The journal of gene medicine*, 3(2), pp. 135–144.

Kim, T. Il *et al.* (2011) 'Bioreducible polymers with cell penetrating and endosome buffering functionality for gene delivery systems', *Journal of Controlled Release*, 152(1), pp. 110–119.

Luzak, B., Siarkiewicz, P. and Boncler, M. (2022) 'An evaluation of a new high-sensitivity PrestoBlue assay for measuring cell viability and drug cytotoxicity using EA.hy926 endothelial cells', *Toxicology in Vitro*, 83, p. 105407.

Männisto, M. *et al.* (2005) 'The role of cell cycle on polyplex-mediated gene transfer into a retinal pigment epithelial cell line', *The Journal of Gene Medicine*, 7(4), pp. 466–476.

Martinez, G. P. *et al.* (2020) 'The Role of Chloroquine and Hydroxychloroquine in Immune Regulation

and Diseases', *Current pharmaceutical design*, 26(35), pp. 4467–4485.

Maugeri, M. *et al.* (2019) 'Linkage between endosomal escape of LNP-mRNA and loading into EVs for transport to other cells', *Nature Communications*, 10(1), pp. 1–15.

Mendes, B. B. *et al.* (2022) 'Nanodelivery of nucleic acids', *Nature Reviews Methods Primers*, 2(1), pp. 1–21.

Merkel, O. M. *et al.* (2011) 'Molecular modeling and in vivo imaging can identify successful flexible triazine dendrimer-based siRNA delivery systems', *Journal of controlled release : official journal of the Controlled Release Society*, 153(1), pp. 23–33.

Miah, K. M., Hyde, S. C. and Gill, D. R. (2019) 'Emerging gene therapies for cystic fibrosis', *Expert Review of Respiratory Medicine*, 13(8), pp. 709–725.

Midoux, P. *et al.* (2008) 'Polymer-based gene delivery: a current review on the uptake and intracellular trafficking of polyplexes', *Current gene therapy*, 8(5), pp. 335–352.

Munson, M. J. *et al.* (2021) 'A high-throughput Galectin-9 imaging assay for quantifying nanoparticle uptake, endosomal escape and functional RNA delivery', *Communications Biology*, 4(1), p. 211.

Patel, S. *et al.* (2017) 'Boosting Intracellular Delivery of Lipid Nanoparticle-Encapsulated mRNA', *Nano letters*, 17(9), pp. 5711–5718.

Paunovska, K. *et al.* (2022) 'Drug delivery systems for RNA therapeutics', *Nature Reviews Genetics*, 23, pp. 265–280.

Pezzoli, D. *et al.* (2017) 'Size matters for in vitro gene delivery: investigating the relationships among complexation protocol, transfection medium, size and sedimentation', *Scientific reports*, 7, p. 44134.

Rashid, M. ur and Coombs, K. M. (2019) 'Serum-reduced media impacts on cell viability and protein expression in human lung epithelial cells', *Journal of Cellular Physiology*, 234(6), p. 7718.

Rejman, J., Bragonzi, A. and Conese, M. (2005) 'Role of clathrin- and caveolae-mediated endocytosis in gene transfer mediated by lipo- and polyplexes', *Molecular therapy : the journal of the American Society of Gene Therapy*, 12(3), pp. 468–474.

Rennick, J., Johnston, A. and Parton, R. (2022) 'Key principles and methods for studying the endocytosis of biological and nanoparticle therapeutics', *Nature Nanotechnology*, 16, pp. 266–276.

Du Rietz, H. *et al.* (2020) 'Imaging small molecule-induced endosomal escape of siRNA', *Nature Communications*, 11(1), pp. 1–17.

Rittner, K. *et al.* (2002) 'New Basic Membrane-Destabilizing Peptides for Plasmid-Based Gene Delivery in Vitro and in Vivo', *Molecular Therapy*, 5(2), pp. 104–114.

Sahay, G. *et al.* (2013) 'Efficiency of siRNA delivery by lipid nanoparticles is limited by endocytic recycling', *Nature biotechnology*, 31(7), pp. 653–658.

Sahin, U. *et al.* (2020) 'An RNA vaccine drives immunity in checkpoint-inhibitor-treated melanoma', *Nature*, 585(7823), pp. 107–112.

Samal, S. K. *et al.* (2012) 'Cationic polymers and their therapeutic potential', *Chemical Society Reviews*, 41(21), pp. 7147–7194.

Shi, L. *et al.* (2021) 'Effects of polyethylene glycol on the surface of nanoparticles for targeted drug delivery', 13, p. 10748.

Silva, I. *et al.* (2022) 'Novel Non-Viral Vectors Based on Pluronic® F68PEI with Application in Oncology

Field', *Polymers 2022, Vol. 14, Page 5315*, 14(23), p. 5315.

Solomon, V. R. and Lee, H. (2009) 'Chloroquine and its analogs: A new promise of an old drug for effective and safe cancer therapies', *European Journal of Pharmacology*, 625(1–3), pp. 220–233.

Tang, G. P. *et al.* (2003) 'Polyethylene glycol modified polyethylenimine for improved CNS gene transfer: effects of PEGylation extent', *Biomaterials*, 24(13), pp. 2351–2362.

Thibault, M. *et al.* (2011) 'Excess polycation mediates efficient chitosan-based gene transfer by promoting lysosomal release of the polyplexes', *Biomaterials*, 32(20), pp. 4639–4646.

Thibault, M. *et al.* (2016) 'Structure Dependence of Lysosomal Transit of Chitosan-Based Polyplexes for Gene Delivery', *Molecular Biotechnology*, 58(10), pp. 648–656.

Ulkoski, D. *et al.* (2021) 'High-Throughput Automation of Endosomolytic Polymers for mRNA Delivery', *ACS Applied Bio Materials*, 4(2), pp. 1640–1654.

Vaidyanathan, S., Orr, B. G. and Banaszak Holl, M. M. (2016) 'Role of Cell Membrane-Vector Interactions in Successful Gene Delivery', *Accounts of Chemical Research*, 49(8), pp. 1486–1493.

Varkouhi, A. K. *et al.* (2011) 'Endosomal escape pathways for delivery of biologicals', *Journal of controlled release : official journal of the Controlled Release Society*, 151(3), pp. 220–228.

Wang, Z. *et al.* (2009) 'Size and dynamics of caveolae studied using nanoparticles in living endothelial cells', *ACS nano*, 3(12), pp. 4110–4116.

Wilschut, K. J. *et al.* (2009) 'Fluorescence in situ hybridization to monitor the intracellular location and accessibility of plasmid DNA delivered by cationic polymer-based gene carriers', *European Journal of Pharmaceutics and Biopharmaceutics*, 72(2), pp. 391–396.

Wu, Z. and Li, T. (2021) 'Nanoparticle-Mediated Cytoplasmic Delivery of Messenger RNA Vaccines: Challenges and Future Perspectives', *Pharmaceutical Research*, 38, pp. 473–478.

Xiang, S. *et al.* (2012) 'Uptake mechanisms of non-viral gene delivery', *Journal of Controlled Release*, 158(3), pp. 371–378.

Yudovin-Farber, I. and Domb, A. J. (2007) 'Cationic polysaccharides for gene delivery', *Materials Science and Engineering*, 27(3), pp. 595-598.

Yue, Y. and Wu, C. (2013) 'Progress and perspectives in developing polymeric vectors for in vitro gene delivery', *Biomaterials Science*, 1(2), pp. 152–170.

Zhang, R. *et al.* (2019) 'Improving cellular uptake of therapeutic entities through interaction with components of cell membrane', *Drug Delivery*, 26(1), p. 328.

Zielínska, A. *et al.* (2020) 'Polymeric Nanoparticles: Production, Characterization, Toxicology and Ecotoxicology', *Molecules*, 25, pp. 1–20.

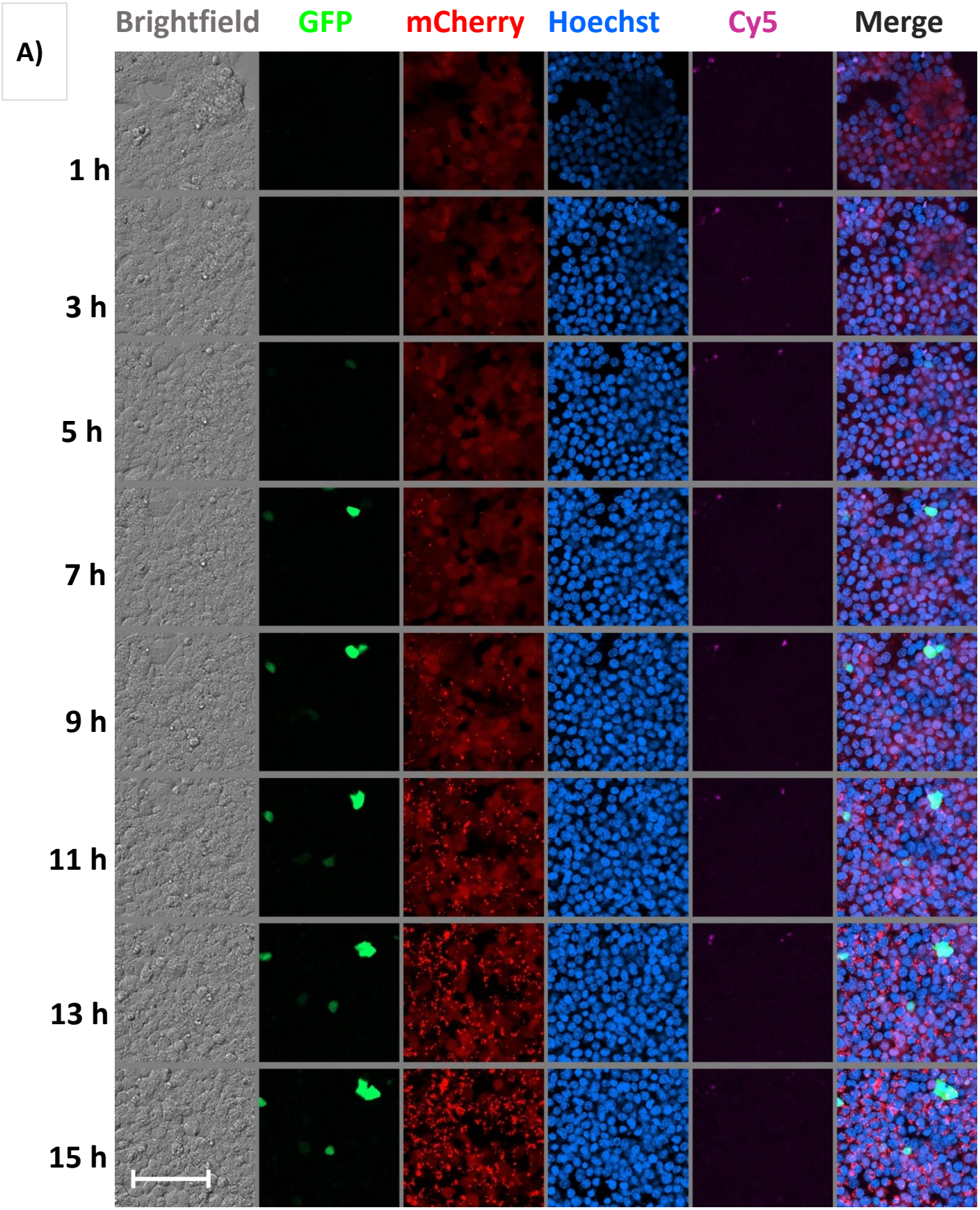
A)
Brightfield
GFP
mCherry
Hoechst
Cy5
Merge
1 h
3 h
5 h
7 h
9 h
11 h
13 h
15 h

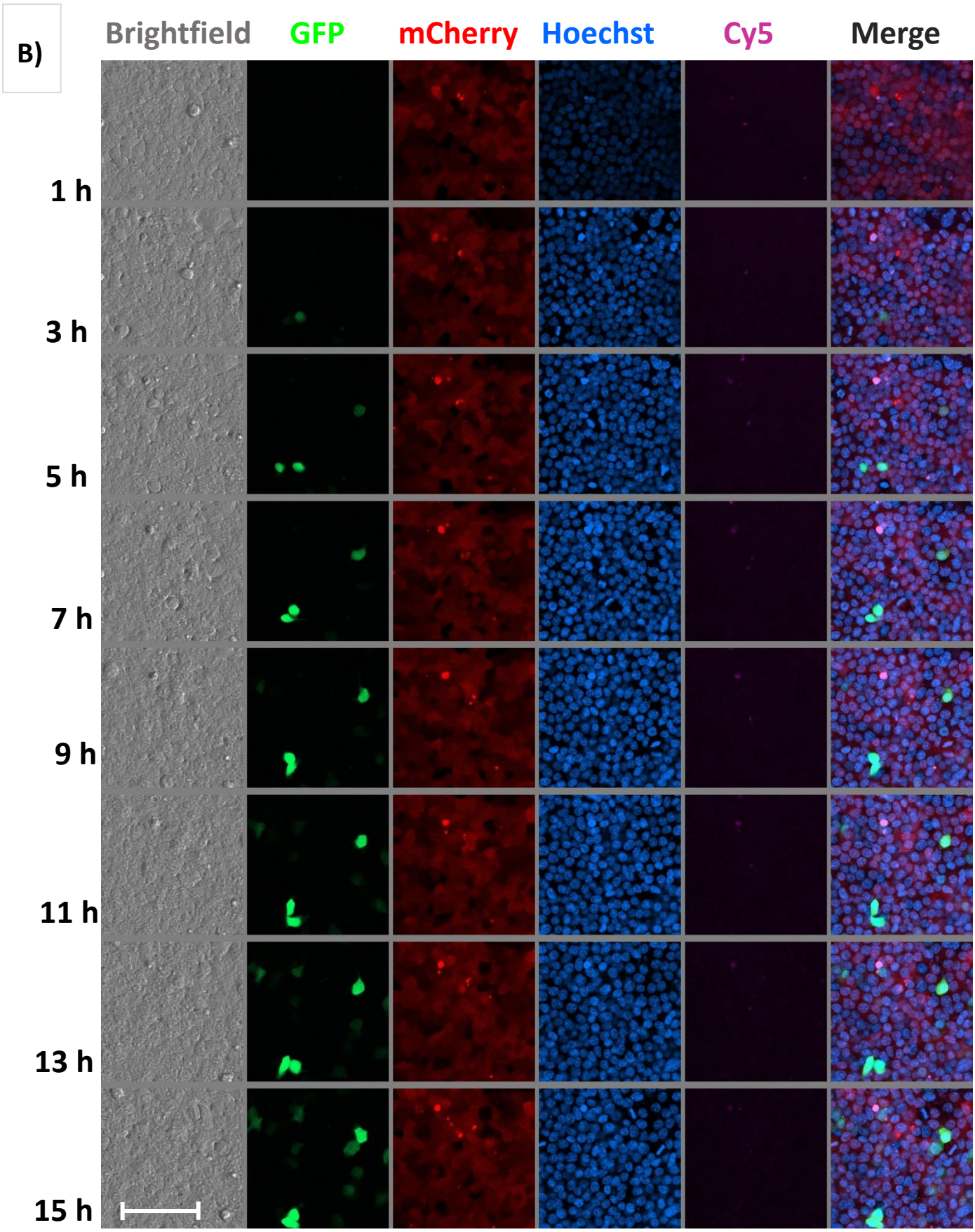

Appendices. 1. *Transfection of mCherry-Gal9 HEK293T cells with TEPA-2L2 N/P 16* ***A)*** *in the presence of Chloroquine (60 µg/mL) and* ***B)*** *in the absence of Chloroquine. Scale bar = 120 µm.*